

Symmetric Galerkin boundary element method for computing the quantum states of the electron in a piecewise-uniform mesoscopic system

Andrea Cagliero¹ and Lyes Rahmouni^{1,2}

¹At the time of the study, both authors were affiliated with the Microwaves Department of IMT Atlantique, Institut Mines-Télécom, and with the Laboratory for Science and Technologies of Information, Communication and Knowledge Lab-STICC (CNRS), Brest, F-29238, France.

²Department of Electronics and Telecommunications, Politecnico di Torino, I-10129 Torino, Italy.

E-mail: andrea.cagliero@edu.unito.it

Abstract. The quantum behavior of charge carriers in semiconductor structures is often described in terms of the effective mass Schrödinger equation, neglecting the rapid fluctuations of the wave function on the scale of the atomic lattice. For systems with piecewise-constant mass and potential energy, this amounts to solving a set of Helmholtz equations with wavenumbers dictated by the physical parameters of each homogeneous subregion. Making use of the Green function method, the system of differential equations can be expressed in boundary integral form to enable efficient numerical solution. In the present study, this strategy is applied in combination with a Galerkin technique to compute the energy spectrum and the wave functions of the electron in a mesoscopic structure composed of two regions. The proposed formulation differs from those presented before for the same scenario in that it implements a symmetric discretization of the four Helmholtz boundary integral operators, which leads to compact expressions and very accurate results.

1. Introduction

In recent years, fundamental and applied research in semiconductor and solid state physics has undergone a significant evolution, with particular emphasis on the study and development of mesoscopic structures and quantum wells [1–3]. Indeed, the quantum confinement of charge carriers is responsible for a rich variety of phenomena that are of interest in optoelectronics, nanotechnology and quantum computing [4]. As it is well-known, the single-particle electronic properties of mesoscopic structures are dictated by the Schrödinger equation and depend on both the electron energy and the confining potential of the atomic lattice. Since for most geometries the energy levels and wave functions of the electron inside such structures cannot be determined analytically, numerical methods are required for both the analysis and interpretation of the experimental results. Among the various computational techniques, the finite element method (FEM) and the boundary element method (BEM) have been explored in the literature [5–10]. Whereas the FEM consists in a volume discretization of the original boundary value problem, the BEM leverages the Green function approach to cast the partial differential equations into a boundary integral form which is then projected on finite dimensional trial spaces. In particular, this last step can be addressed by collocation, explicitly imposing the boundary integral equations at a finite set of points, or by the Galerkin approach, where the equations are enforced in a weighted average sense [11]. The main limitation of the BEM is that it requires the knowledge of the Green function of the physical system: for arbitrary confining potentials, the Green

function cannot be expressed in closed form. However, mesoscopic structures are often constituted by piecewise-homogeneous regions, which means that only free-space Green functions are needed. In this case, owing to the reduction in dimensionality, the BEM is often more efficient than the FEM; moreover, the BEM provides a very natural strategy to compute the scattering of the electron wave function into unbounded regions. Although most of the literature deals primarily with collocation methods, the Galerkin BEM is known to be more accurate and robust.

In this work, a BEM involving the Galerkin discretization of the matrix integral operator (30) is proposed to solve the effective mass Schrödinger equation (Section 2) for a charge carrier in a mesoscopic system comprising two regions with piecewise-constant mass and potential energy. The formulation enables the determination of the discrete energy levels (Section 3), the scattering amplitudes (Section 4) and the spectral density of the system (Section 5), as well as the corresponding wave functions. For the reader's benefit, the paper is self-contained and in Appendix A, Appendix B and Appendix C some technical details of the BEM derivation are reminded to the reader and adapted to the notation of the main text. Additional results and insights can be found in Appendix D and in Appendix E.

2. Problem statement

Let us consider the non-relativistic time-dependent Schrödinger equation for the electron wave function within an arbitrary mesoscopic structure [2]. Under the effective mass approximation for the envelope function $\Psi(\mathbf{r}, t)$, the equation reads:

$$i\hbar \frac{\partial \Psi(\mathbf{r}, t)}{\partial t} = -\frac{\hbar^2}{2} \nabla \cdot \left[\frac{1}{m(\mathbf{r})} \nabla \Psi(\mathbf{r}, t) \right] + V(\mathbf{r}) \Psi(\mathbf{r}, t), \quad (1)$$

being $m(\mathbf{r})$ the electron mass [12] and $V(\mathbf{r})$ the potential energy of the confining structure. Assuming a time-harmonic dependence of the form:

$$\Psi(\mathbf{r}, t) = \psi(\mathbf{r}) \exp\left(-i\frac{E}{\hbar}t\right), \quad (2)$$

where E represents the electron energy, equation (1) is reduced to:

$$\frac{\hbar^2}{2} \nabla \cdot \left[\frac{1}{m(\mathbf{r})} \nabla \psi(\mathbf{r}) \right] + [E - V(\mathbf{r})] \psi(\mathbf{r}) = 0. \quad (3)$$

For piecewise constant mass and potential energy, the previous expression can be put in the same form as the scalar Helmholtz equation [5–8]. Suppose, for instance, that the mesoscopic structure can be divided into N homogeneous subregions Ω_j such that $m(\mathbf{r}) = m_j$ and $V(\mathbf{r}) = V_j$ for $\mathbf{r} \in \Omega_j$, where j runs from 1 to N . Within the j -th subregion, equation (3) becomes:

$$\frac{\hbar^2}{2m_j} \Delta \psi(\mathbf{r}) + (E - V_j) \psi(\mathbf{r}) = 0 \quad \mathbf{r} \in \Omega_j. \quad (4)$$

Here and below, the symbol Δ stands for the Laplacian. Making use of the following definition:

$$k_j^2 \equiv \frac{2m_j}{\hbar^2} (E - V_j), \quad (5)$$

we finally obtain:

$$\Delta \psi(\mathbf{r}) + k_j^2 \psi(\mathbf{r}) = 0 \quad \mathbf{r} \in \Omega_j. \quad (6)$$

For each wavenumber k_j , the unique form of the free-space Green function $g_j(\mathbf{r}, \mathbf{r}')$ satisfying:

$$\Delta g_j(\mathbf{r}, \mathbf{r}') + k_j^2 g_j(\mathbf{r}, \mathbf{r}') = -\delta(\mathbf{r} - \mathbf{r}') \quad (7)$$

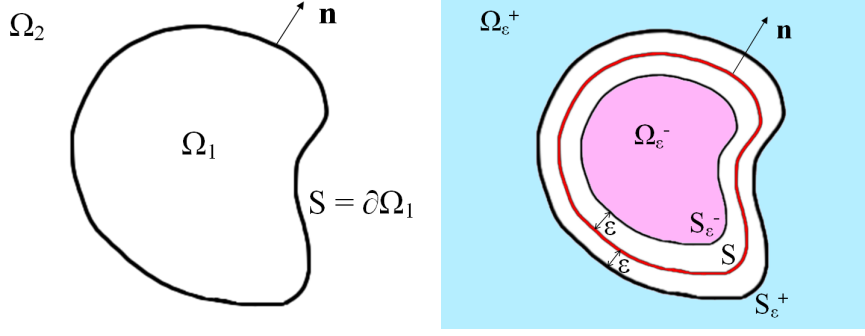


Figure 1. *Left:* sketch of the geometry of the problem. *Right:* two parallel surfaces S_ϵ^\pm .

and the Sommerfeld radiation condition:

$$\left| \frac{\mathbf{r}}{|\mathbf{r}|} \cdot \nabla g_j(\mathbf{r}, \mathbf{r}') - ik_j g_j(\mathbf{r}, \mathbf{r}') \right| = O\left(\frac{1}{|\mathbf{r}|^2}\right) \quad |\mathbf{r}| \rightarrow \infty \quad (8)$$

will be considered, according to the usual convention. It is important to note that, for the kinetic energy operator to be Hermitian, both the wave function ψ and its weighted normal derivative $m^{-1}\partial_n\psi$ must be continuous across the interface between any two different subregions [12]. In the next sections, these boundary conditions are used together with (8) to solve equation (6) numerically by the symmetric Galerkin BEM for $N = 2$ homogeneous subregions.

3. Bound states

3.1. Integral equations

As a general example, let $\Omega_1 \subset \mathbb{R}^n$ with $n = 1, 2$ or 3 be a finite spatial region enclosed by a boundary $S = \partial\Omega_1$ with outward pointing normal \mathbf{n} and let $\Omega_2 = \mathbb{R}^n \setminus \bar{\Omega}_1$ be the exterior region (see Figure 1, left side). Assuming a potential energy and an electron mass, respectively, of the form:

$$V(\mathbf{r}) = \begin{cases} 0 & \mathbf{r} \in \Omega_1; \\ V & \mathbf{r} \in \Omega_2, \end{cases} \quad m(\mathbf{r}) = \begin{cases} m_1 & \mathbf{r} \in \Omega_1; \\ m_2 & \mathbf{r} \in \Omega_2, \end{cases} \quad (9)$$

with V , m_1 and m_2 constants, equation (6) can be rewritten as:

$$\begin{cases} \Delta\psi(\mathbf{r}) + k_1^2\psi(\mathbf{r}) = 0 & \mathbf{r} \in \Omega_1; \\ \Delta\psi(\mathbf{r}) + k_2^2\psi(\mathbf{r}) = 0 & \mathbf{r} \in \Omega_2, \end{cases} \quad (10)$$

where:

$$k_1^2 = \frac{2m_1}{\hbar^2}E, \quad k_2^2 = \frac{2m_2}{\hbar^2}(E - V). \quad (11)$$

Let us represent the total electron wave function $\psi(\mathbf{r})$ as follows:

$$\psi(\mathbf{r}) \equiv \begin{cases} \psi_1(\mathbf{r}) & \mathbf{r} \in \Omega_1; \\ \psi_2(\mathbf{r}) & \mathbf{r} \in \Omega_2. \end{cases} \quad (12)$$

With this notation, (10) becomes:

$$\Delta\psi_j(\mathbf{r}) + k_j^2\psi_j(\mathbf{r}) = 0 \quad j = 1, 2. \quad (13)$$

Denoting by $g_1(\mathbf{r}, \mathbf{r}')$ and $g_2(\mathbf{r}, \mathbf{r}')$ the free-space Green functions in the two regions, we have:

$$\Delta g_j(\mathbf{r}, \mathbf{r}') + k_j^2 g_j(\mathbf{r}, \mathbf{r}') = -\delta(\mathbf{r} - \mathbf{r}') \quad j = 1, 2. \quad (14)$$

If we make the replacement $\mathbf{r} \leftrightarrow \mathbf{r}'$ in (13) and (14), multiply the first expression by $g_j(\mathbf{r}, \mathbf{r}')$, the second by $\psi_j(\mathbf{r}')$ and finally compute the difference between the two, we arrive at:

$$g_j \Delta' \psi_j(\mathbf{r}') - \psi_j(\mathbf{r}') \Delta' g_j = \psi_j(\mathbf{r}') \delta(\mathbf{r} - \mathbf{r}') \quad j = 1, 2, \quad (15)$$

where the argument $(\mathbf{r}, \mathbf{r}')$ of the Green function has been suppressed for brevity. Let us first consider the case $\mathbf{r} \notin S$. By performing the integration of (15) in $d\mathbf{r}'$ over the volume $\Omega_j \setminus B_\varrho(\mathbf{r})$, where $B_\varrho(\mathbf{r})$ is a ball of radius ϱ and center $\mathbf{r} \in \Omega_j$, making use of the following Green's identity:

$$\int_{\Omega} d\mathbf{r}' [g \Delta' \psi(\mathbf{r}') - \psi(\mathbf{r}') \Delta' g] = \int_{\partial\Omega} d\mathbf{r}' \left[g \frac{\partial \psi(\mathbf{r}')}{\partial n'} - \psi(\mathbf{r}') \frac{\partial g}{\partial n'} \right], \quad (16)$$

where $\partial/\partial n' = \mathbf{n}' \cdot \nabla'$ is the derivative with respect to the outward pointing normal to the integration surface computed at \mathbf{r}' , and taking the limit $\varrho \rightarrow 0$, we get:

$$\int_S d\mathbf{r}' \left[g_j \frac{\partial \psi_j(\mathbf{r}')}{\partial n'} - \psi_j(\mathbf{r}') \frac{\partial g_j}{\partial n'} \right] \mp \lim_{\varrho \rightarrow 0} \int_{\partial B_\varrho(\mathbf{r})} d\mathbf{r}' \left[g_j \frac{\partial \psi_j(\mathbf{r}')}{\partial n'} - \psi_j(\mathbf{r}') \frac{\partial g_j}{\partial n'} \right] = 0 \quad j = 1, 2. \quad (17)$$

As it is shown in Appendix A, the second term in (17) reduces to:

$$\lim_{\varrho \rightarrow 0} \int_{\partial B_\varrho(\mathbf{r})} d\mathbf{r}' \left[g_j \frac{\partial \psi_j(\mathbf{r}')}{\partial n'} - \psi_j(\mathbf{r}') \frac{\partial g_j}{\partial n'} \right] = \psi_j(\mathbf{r}) \quad j = 1, 2, \quad (18)$$

so that we are left with:

$$\begin{cases} \psi_1(\mathbf{r}) = \int_S d\mathbf{r}' \left[g_1 \frac{\partial \psi_1(\mathbf{r}')}{\partial n'} - \psi_1(\mathbf{r}') \frac{\partial g_1}{\partial n'} \right] & \mathbf{r} \in \Omega_1; \\ \psi_2(\mathbf{r}) = \int_S d\mathbf{r}' \left[g_2 \frac{\partial \psi_2(\mathbf{r}')}{\partial n'} - \psi_2(\mathbf{r}') \frac{\partial g_2}{\partial n'} \right] & \mathbf{r} \in \Omega_2. \end{cases} \quad (19)$$

In deriving the second equation in (19), the Sommerfeld radiation condition (8) has been used in order to neglect the contribution at infinity. Taking $f(\cdot)$ to represent $\psi(\cdot)$, $g(\mathbf{r}, \cdot)$ and their normal derivative, the evaluation of the integrand functions at any point \mathbf{r}_S on the boundary should be conceived as follows¹:

$$f_1(\mathbf{r}_S) \equiv \lim_{\varepsilon \rightarrow 0} f_1(\mathbf{r}_S - \varepsilon \mathbf{n}), \quad f_2(\mathbf{r}_S) \equiv \lim_{\varepsilon \rightarrow 0} f_2(\mathbf{r}_S + \varepsilon \mathbf{n}). \quad (20)$$

The same strategy can be used to obtain the limiting values of (19) for $\mathbf{r} \in S$. In one dimension, where the boundary integrals are replaced by point evaluations, this poses no problem. Conversely, owing to the singularity of the Green functions, special care must be taken to address the two-dimensional and three-dimensional cases. In particular, by deforming the boundary integrals so that \mathbf{r} still resides inside Ω_j , it can be shown that (see Appendix B)²:

$$\begin{cases} \frac{\psi_1(\mathbf{r})}{2} = f_S \int_S d\mathbf{r}' \left[g_1 \frac{\partial \psi_1(\mathbf{r}')}{\partial n'} - \psi_1(\mathbf{r}') \frac{\partial g_1}{\partial n'} \right] & \mathbf{r} \in S; \\ \frac{\psi_2(\mathbf{r})}{2} = f_S \int_S d\mathbf{r}' \left[g_2 \frac{\partial \psi_2(\mathbf{r}')}{\partial n'} - \psi_2(\mathbf{r}') \frac{\partial g_2}{\partial n'} \right] & \mathbf{r} \in S, \end{cases} \quad (21)$$

¹ In order to avoid abuse of notation, the normal derivatives must be computed on the surfaces defined by $\mathbf{r}_S - \varepsilon \mathbf{n}$ and $\mathbf{r}_S + \varepsilon \mathbf{n}$, respectively.

² An alternative derivation would require to apply again (15) and (16) integrating over $\Omega_j \setminus [\Omega_j \cap B_\varrho(\mathbf{r}_S)]$.

where the symbol f stands for the Cauchy principal value integral.

We now introduce the boundary conditions for the wave function. First, let us define:

$$\chi_j(\mathbf{r}_S) \equiv \frac{1}{m_j} \frac{\partial \psi_j(\mathbf{r}_S)}{\partial n} \quad j = 1, 2. \quad (22)$$

With this convention, and taking into account (20), the continuity of the electron wave function and of its normal derivative at the boundary S can be expressed as:

$$\begin{cases} \delta\psi(\mathbf{r}_S) \equiv \psi_2(\mathbf{r}_S) - \psi_1(\mathbf{r}_S) = 0 & \Rightarrow \psi_2(\mathbf{r}_S) = \psi_1(\mathbf{r}_S) \equiv \psi(\mathbf{r}_S); \\ \delta\chi(\mathbf{r}_S) \equiv \chi_2(\mathbf{r}_S) - \chi_1(\mathbf{r}_S) = 0 & \Rightarrow \chi_2(\mathbf{r}_S) = \chi_1(\mathbf{r}_S) \equiv \chi(\mathbf{r}_S). \end{cases} \quad (23)$$

System (21) is then reduced to:

$$\begin{cases} \frac{\psi(\mathbf{r}_S)}{2} + \oint_S d\mathbf{r}'_S \left[\frac{\partial g_1(\mathbf{r}_S, \mathbf{r}'_S)}{\partial n'} \psi(\mathbf{r}'_S) - m_1 g_1(\mathbf{r}_S, \mathbf{r}'_S) \chi(\mathbf{r}'_S) \right] = 0; \\ \frac{\psi(\mathbf{r}_S)}{2} + \oint_S d\mathbf{r}'_S \left[-\frac{\partial g_2(\mathbf{r}_S, \mathbf{r}'_S)}{\partial n'} \psi(\mathbf{r}'_S) + m_2 g_2(\mathbf{r}_S, \mathbf{r}'_S) \chi(\mathbf{r}'_S) \right] = 0 \end{cases} \quad (24)$$

and, by subtracting the two equations, we arrive at:

$$\oint_S d\mathbf{r}'_S \left[\frac{\partial g_1(\mathbf{r}_S, \mathbf{r}'_S)}{\partial n'} + \frac{\partial g_2(\mathbf{r}_S, \mathbf{r}'_S)}{\partial n'} \right] \psi(\mathbf{r}'_S) - \oint_S d\mathbf{r}'_S [m_1 g_1(\mathbf{r}_S, \mathbf{r}'_S) + m_2 g_2(\mathbf{r}_S, \mathbf{r}'_S)] \chi(\mathbf{r}'_S) = 0. \quad (25)$$

Let us now consider the following families of parallel surfaces:

$$S_\varepsilon^- \equiv \{\mathbf{r} \in \Omega_1 : \mathbf{r} = \mathbf{r}_S - \varepsilon \mathbf{n}, \mathbf{r}_S \in S\}, \quad S_\varepsilon^+ \equiv \{\mathbf{r} \in \Omega_2 : \mathbf{r} = \mathbf{r}_S + \varepsilon \mathbf{n}, \mathbf{r}_S \in S\}, \quad (26)$$

denote by \mathbf{n}_\mp the corresponding outward pointing normals, by $\Omega_\varepsilon^- \subset \Omega_1$ the inner volume with respect to S_ε^- and by $\Omega_\varepsilon^+ \subset \Omega_2$ the outer volume with respect to S_ε^+ (see Figure 1, right side). On computing the normal derivative of (19) at S_ε^\mp , respectively, we get:

$$\begin{cases} \frac{\partial \psi_1(\mathbf{r})}{\partial n_-} = \int_S d\mathbf{r}' \left[\frac{\partial g_1}{\partial n_-} \frac{\partial \psi_1(\mathbf{r}')}{\partial n'} - \psi_1(\mathbf{r}') \frac{\partial^2 g_1}{\partial n_- \partial n'} \right] & \mathbf{r} \in S_\varepsilon^-; \\ \frac{\partial \psi_2(\mathbf{r})}{\partial n_+} = \int_S d\mathbf{r}' \left[\psi_2(\mathbf{r}') \frac{\partial^2 g_2}{\partial n_+ \partial n'} - \frac{\partial g_2}{\partial n_+} \frac{\partial \psi_2(\mathbf{r}')}{\partial n'} \right] & \mathbf{r} \in S_\varepsilon^+. \end{cases} \quad (27)$$

Dividing the first equation by m_1 , the second by m_2 and taking the difference between the two under the limit $\varepsilon \rightarrow 0$ gives (see Appendix C):

$$\int_S d\mathbf{r}'_S \left[\frac{1}{m_1} \frac{\partial^2 g_1(\mathbf{r}_S, \mathbf{r}'_S)}{\partial n \partial n'} + \frac{1}{m_2} \frac{\partial^2 g_2(\mathbf{r}_S, \mathbf{r}'_S)}{\partial n \partial n'} \right] \psi(\mathbf{r}'_S) - \int_S d\mathbf{r}'_S \left[\frac{\partial g_1(\mathbf{r}_S, \mathbf{r}'_S)}{\partial n} + \frac{\partial g_2(\mathbf{r}_S, \mathbf{r}'_S)}{\partial n} \right] \chi(\mathbf{r}'_S) = 0. \quad (28)$$

It is fundamental to keep in mind that the first integral in (28) is hypersingular and does not exist as Cauchy principal value.

Equations (25) and (28) can be rewritten more concisely as:

$$\hat{\mathbf{H}} \begin{bmatrix} \psi \\ \chi \end{bmatrix}(\mathbf{r}_S) = 0, \quad (29)$$

where the operator $\hat{\mathbf{H}}$ is expressed in matrix form (here we adapt the notation of [13] to the present scenario):

$$\hat{\mathbf{H}} \equiv \begin{pmatrix} -\hat{D} & \hat{S} \\ -\hat{N} & \hat{D}^\dagger \end{pmatrix} \quad (30)$$

with entries defined as boundary integral operators over an arbitrary wave function $f(\mathbf{r})$:

$$\hat{S}[f](\mathbf{r}_S) \equiv \int_S d\mathbf{r}'_S [m_1 g_1(\mathbf{r}_S, \mathbf{r}'_S) + m_2 g_2(\mathbf{r}_S, \mathbf{r}'_S)] f(\mathbf{r}'_S); \quad (31)$$

$$\hat{D}[f](\mathbf{r}_S) \equiv \int_S d\mathbf{r}'_S \left[\frac{\partial g_1(\mathbf{r}_S, \mathbf{r}'_S)}{\partial n'} + \frac{\partial g_2(\mathbf{r}_S, \mathbf{r}'_S)}{\partial n'} \right] f(\mathbf{r}'_S); \quad (32)$$

$$\hat{D}^\dagger[f](\mathbf{r}_S) \equiv \int_S d\mathbf{r}'_S \left[\frac{\partial g_1(\mathbf{r}_S, \mathbf{r}'_S)}{\partial n} + \frac{\partial g_2(\mathbf{r}_S, \mathbf{r}'_S)}{\partial n} \right] f(\mathbf{r}'_S); \quad (33)$$

$$\hat{N}[f](\mathbf{r}_S) \equiv \int_S d\mathbf{r}'_S \left[\frac{1}{m_1} \frac{\partial^2 g_1(\mathbf{r}_S, \mathbf{r}'_S)}{\partial n \partial n'} + \frac{1}{m_2} \frac{\partial^2 g_2(\mathbf{r}_S, \mathbf{r}'_S)}{\partial n \partial n'} \right] f(\mathbf{r}'_S). \quad (34)$$

To summarize, the solution of the original Schrödinger equation in the two regions has been rewritten through (19) and (23) as an integral expression involving the values of the functions ψ and χ at the boundary:

$$\begin{cases} \psi_1(\mathbf{r}) = \int_S d\mathbf{r}'_S \left[m_1 g_1(\mathbf{r}, \mathbf{r}'_S) \chi(\mathbf{r}'_S) - \frac{\partial g_1(\mathbf{r}, \mathbf{r}'_S)}{\partial n'} \psi(\mathbf{r}'_S) \right] & \mathbf{r} \in \Omega_1; \\ \psi_2(\mathbf{r}) = \int_S d\mathbf{r}'_S \left[\frac{\partial g_2(\mathbf{r}, \mathbf{r}'_S)}{\partial n'} \psi(\mathbf{r}'_S) - m_2 g_2(\mathbf{r}, \mathbf{r}'_S) \chi(\mathbf{r}'_S) \right] & \mathbf{r} \in \Omega_2. \end{cases} \quad (35)$$

In (29), the boundary restrictions $\psi(\mathbf{r}_S)$ and $\chi(\mathbf{r}_S)$ are found to span the null space of the matrix integral operator (30). It is important to note that the \hat{S} , \hat{D} , \hat{D}^\dagger and \hat{N} operators are coercive [16] but they may lack injectivity for some discrete values of the electron energy depending on the geometry and physical parameters of the system: those energies constitute the bound portion of the spectrum. The bound states of the quantum problem are intimately related to the resonant modes of the corresponding Helmholtz problem, with the presence in both cases of a non-trivial null space of the BEM operator.

3.2. Discretization of the operators

In order to solve numerically the above derived integral equations, the boundary S is discretized into a collection of simplices $\{S_n\}$ (segments and triangles in two and three dimensions, respectively). We then expand the unknowns ψ and χ in (29) on a set of node-based basis functions $\{f_j\}$ as follows:

$$\psi(\mathbf{r}'_S) = \sum_j \alpha_j f_j(\mathbf{r}'_S); \quad \chi(\mathbf{r}'_S) = \mu^{-1} \sum_j \beta_j f_j(\mathbf{r}'_S), \quad (36)$$

being μ a dimensionless constant with the same order of magnitude as the electron mass, used to avoid scaling issues in the numeric computation. The j -th basis function is defined on the set of simplices $\{S_n\}$ that share the j -th mesh node, hereinafter referred to as $\{n \in j\}$, and vanishes out of its defining domain, so that:

$$\int_S d\mathbf{r}'_S f_j(\mathbf{r}'_S) = \sum_{n \in j} \int_{S_n} d\mathbf{r}' f_j^n(\mathbf{r}'), \quad (37)$$

with f_j^n representing the restriction of the basis function to the n -th simplex. Following the Galerkin approach [11], we multiply equation (29) by $f_i(\mathbf{r}_S)$ and integrate over S to obtain:

$$\sum_j \mathbf{H}_{ij} \begin{bmatrix} \alpha_j \\ \beta_j \end{bmatrix} = 0, \quad (38)$$

where:

$$\mathbf{H}_{ij} \equiv \begin{pmatrix} -D_{ij} & \mu^{-1} S_{ij} \\ -\mu N_{ij} & D_{ij}^\dagger \end{pmatrix} \quad (39)$$

and the discrete boundary operators are given by:

$$S_{ij} \equiv \sum_{m \in i} \sum_{n \in j} \int_{S_m} d\mathbf{r} \int_{S_n} d\mathbf{r}' [m_1 g_1(\mathbf{r}, \mathbf{r}') + m_2 g_2(\mathbf{r}, \mathbf{r}')] f_i^m(\mathbf{r}) f_j^n(\mathbf{r}'); \quad (40)$$

$$D_{ij} \equiv \sum_{m \in i} \sum_{n \in j} \int_{S_m} d\mathbf{r} \int_{S_n} d\mathbf{r}' \left[\frac{\partial g_1(\mathbf{r}, \mathbf{r}')}{\partial n'} + \frac{\partial g_2(\mathbf{r}, \mathbf{r}')}{\partial n'} \right] f_i^m(\mathbf{r}) f_j^n(\mathbf{r}'); \quad (41)$$

$$D_{ij}^\dagger \equiv \sum_{m \in i} \sum_{n \in j} \int_{S_m} d\mathbf{r} \int_{S_n} d\mathbf{r}' \left[\frac{\partial g_1(\mathbf{r}, \mathbf{r}')}{\partial n} + \frac{\partial g_2(\mathbf{r}, \mathbf{r}')}{\partial n} \right] f_i^m(\mathbf{r}) f_j^n(\mathbf{r}'); \quad (42)$$

$$N_{ij} \equiv \sum_{m \in i} \sum_{n \in j} \int_{S_m} d\mathbf{r} \int_{S_n} d\mathbf{r}' \left[\frac{1}{m_1} \frac{\partial^2 g_1(\mathbf{r}, \mathbf{r}')}{\partial n \partial n'} + \frac{1}{m_2} \frac{\partial^2 g_2(\mathbf{r}, \mathbf{r}')}{\partial n \partial n'} \right] f_i^m(\mathbf{r}) f_j^n(\mathbf{r}'). \quad (43)$$

When the simplices S_m and S_n do not share any vertex, the matrix entries (40)-(43) can be easily computed by Gauss-Legendre quadrature rules [14]. Conversely, owing to the singularity of the Green functions and their normal derivatives, most integrations over coincident and adjacent elements require the use of regularization techniques (see, for instance, [15]). Following the variational formulation proposed in [13] and [16], the hypersingular matrix (43) may be replaced by a discrete version of the bilinear form induced by the corresponding single layer potential, which proves similar to (40) and easier to deal with. In Appendix D, quasi-closed-form expressions are provided for the coincident integrations appearing throughout (40)-(43) in the two-dimensional case with first-order basis functions. To the best of our knowledge, these formulas are applied here for the first time.

Once the above matrices are computed, the sets of expansion coefficients $\{\alpha_j\}$ and $\{\beta_j\}$ can be estimated by solving (38) numerically, and this in turn leads to the determination of the boundary unknowns $\psi(\mathbf{r}_S)$ and $\chi(\mathbf{r}_S)$ via (36). Since the matrix entries depend parametrically on the energy E of the electron, root-finding methods must be employed to localize the bound states, seeking for those specific eigenenergies that lead to a vanishing determinant of the block matrix (39). Finally, from (35), (36) and (37), we arrive at the BEM solution:

$$\begin{cases} \psi_1(\mathbf{r}) = \sum_j \sum_{n \in j} \int_{S_n} d\mathbf{r}' \left[\beta_j \frac{m_1}{\mu} g_1(\mathbf{r}, \mathbf{r}') - \alpha_j \frac{\partial g_1(\mathbf{r}, \mathbf{r}')}{\partial n'} \right] f_j^n(\mathbf{r}') & \mathbf{r} \in \Omega_1; \\ \psi_2(\mathbf{r}) = \sum_j \sum_{n \in j} \int_{S_n} d\mathbf{r}' \left[\alpha_j \frac{\partial g_2(\mathbf{r}, \mathbf{r}')}{\partial n'} - \beta_j \frac{m_2}{\mu} g_2(\mathbf{r}, \mathbf{r}') \right] f_j^n(\mathbf{r}') & \mathbf{r} \in \Omega_2, \end{cases} \quad (44)$$

which can be more usefully expressed as:

$$\begin{cases} \psi_1(\mathbf{r}) = \sum_n \int_{S_n} d\mathbf{r}' \sum_{j \in n} \left[\beta_j \frac{m_1}{\mu} g_1(\mathbf{r}, \mathbf{r}') - \alpha_j \frac{\partial g_1(\mathbf{r}, \mathbf{r}')}{\partial n'} \right] f_j^n(\mathbf{r}') & \mathbf{r} \in \Omega_1; \\ \psi_2(\mathbf{r}) = \sum_n \int_{S_n} d\mathbf{r}' \sum_{j \in n} \left[\alpha_j \frac{\partial g_2(\mathbf{r}, \mathbf{r}')}{\partial n'} - \beta_j \frac{m_2}{\mu} g_2(\mathbf{r}, \mathbf{r}') \right] f_j^n(\mathbf{r}') & \mathbf{r} \in \Omega_2, \end{cases} \quad (45)$$

being $\{j \in n\}$ the set of mesh nodes that belong to the n -th simplex.

3.3. Examples and comparisons

With reference to [5], let us first consider a stadium-shaped boundary of size $50 \times 25 \text{ nm}^2$ with a potential offset $V = 10 \text{ meV}$ and take the electron effective mass to be $0.0665 m_e$ in both the inner and outer regions, where $m_e \approx 9.11 \times 10^{-31} \text{ Kg}$ represents the electron rest mass. The contour plots of the two bound electron states computed by the proposed BEM are shown in Figure 2, whereas the corresponding energies are reported in Table 1 for different numbers of mesh elements \mathcal{N} . From this analysis, the relative error of the calculated energies is found to decrease as $O(\mathcal{N}^{-2})$. As a further comparison, the contour plot of the excited electron state at 184.4 meV , computed using $V = 190 \text{ meV}$, is displayed in Figure 3. The results are in good agreement with those presented in [5].

The stadium is now replaced by a rectangular boundary of the same size. When the potential offset V in (9) tends to infinity, the electron wave function in the outer region vanishes and the Schrödinger

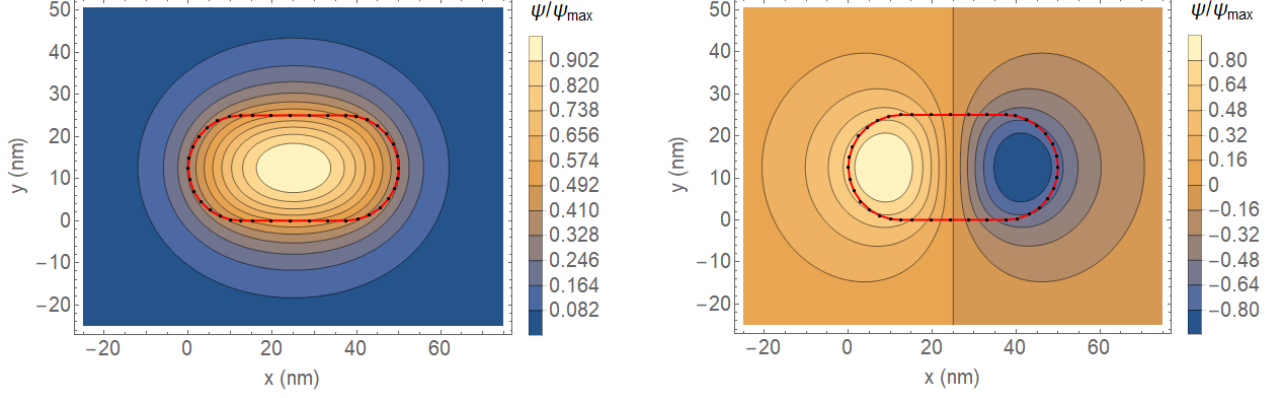


Figure 2. Contour plots of the two bound electron wave functions in a stadium-shaped structure of size $50 \times 25 \text{ nm}^2$ with $m_1 = m_2 = 0.0665 m_e$ and $V = 10 \text{ meV}$. The wave functions are computed by the proposed BEM formulation via (38) and (45) using a mesh of 40 elements, first-order basis functions and a 10 points Gauss-Legendre quadrature for the numerical integrations.

number of mesh elements	first energy level (meV)	second energy level (meV)
16	4.8494	8.7556
24	4.8255	8.6924
32	4.8128	8.6588
40	4.8090	8.6496
50	4.8074	8.6443
100	4.8023	8.6325
200	4.8021	8.6305

Table 1. BEM-computed energies of the two bound electron states in a stadium-shaped structure with the same parameters as in Figure 2. The energies are obtained minimizing the function $|\det \mathbf{H}(E)|$ by standard root-finding algorithms.

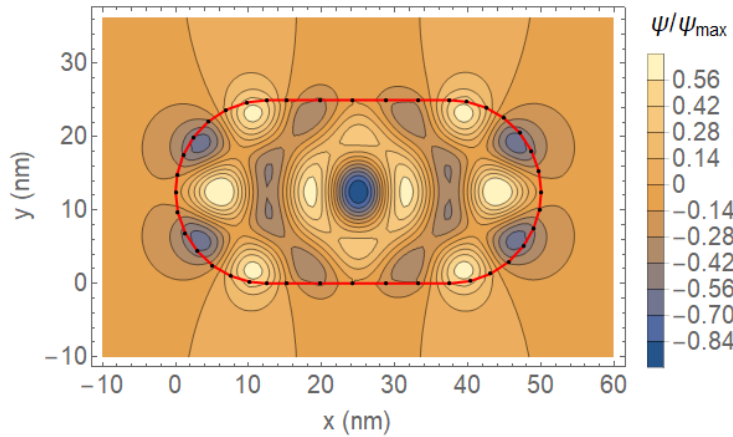


Figure 3. Contour plot of the electron wave function in a stadium-shaped structure of size $50 \times 25 \text{ nm}^2$ with $m_1 = m_2 = 0.0665 m_e$, $E = 184.4 \text{ meV}$ and $V = 190 \text{ meV}$. The wave function is computed by the proposed BEM formulation via (38) and (45) using a mesh of 40 elements, first-order basis functions and a 10 points Gauss-Legendre quadrature for the numerical integrations.

equation for the inner region can be solved very easily by separation of variables. Imposing the continuity of the wave function at the boundary and the normalization condition, we obtain:

$$\begin{cases} \psi_1^{(\infty)}(x, y) = \sqrt{\frac{2}{L_x}} \sin\left(\frac{n_x \pi x}{L_x}\right) \sqrt{\frac{2}{L_y}} \sin\left(\frac{n_y \pi y}{L_y}\right) & (x, y) \in \Omega_1; \\ \psi_2^{(\infty)}(x, y) = 0 & (x, y) \in \Omega_2, \end{cases} \quad (46)$$

where $n_x, n_y \in \mathbb{Z}$ are the quantum numbers and L_x, L_y represent the sides of the rectangle. The energy of the confined states can then be expressed analytically as follows:

$$E_{n_x n_y}^{(\infty)} = \frac{\hbar^2 \pi^2}{2m} \left(\frac{n_x^2}{L_x^2} + \frac{n_y^2}{L_y^2} \right). \quad (47)$$

In the present scenario, the infinite potential offset breaks the continuity of the normal derivative of the wave function across the boundary and leads to a vanishing Green function in the outer region, so that system (19) reduces to:

$$\begin{cases} \psi_1(\mathbf{r}) = \int_S d\mathbf{r}'_S g_1(\mathbf{r}, \mathbf{r}'_S) \frac{\partial \psi_1(\mathbf{r}'_S)}{\partial n'} & \mathbf{r} \in \Omega_1; \\ \psi_2(\mathbf{r}) = 0 & \mathbf{r} \in \Omega_2 \end{cases} \quad (48)$$

and the boundary conditions (23) are replaced by:

$$\psi_2(\mathbf{r}_S) = \psi_1(\mathbf{r}_S) \equiv \psi(\mathbf{r}_S) = 0. \quad (49)$$

Despite the BEM equations derived in the previous sections no longer hold, we can still use (48) and (49) to express a simplified boundary integral equation only involving the normal derivative of the wave function:

$$\hat{\mathbf{s}}_1 \left[\frac{\partial \psi_1}{\partial n} \right] (\mathbf{r}_S) \equiv \oint_S d\mathbf{r}'_S g_1(\mathbf{r}_S, \mathbf{r}'_S) \frac{\partial \psi_1(\mathbf{r}'_S)}{\partial n'} = 0, \quad (50)$$

which is discretized as usual:

$$\frac{\partial \psi_1(\mathbf{r}'_S)}{\partial n'} = \sum_j \beta_j f_j(\mathbf{r}'_S); \quad \sum_j (\mathbf{s}_1)_{ij} \beta_j = 0; \quad (51)$$

$$(\mathbf{s}_1)_{ij} \equiv \sum_{m \in i} \sum_{n \in j} \int_{S_m} d\mathbf{r} \int_{S_n} d\mathbf{r}' g_1(\mathbf{r}, \mathbf{r}') f_i^m(\mathbf{r}) f_j^n(\mathbf{r}'); \quad (52)$$

$$\psi_1(\mathbf{r}) = \sum_n \int_{S_n} d\mathbf{r}' g_1(\mathbf{r}, \mathbf{r}') \sum_{j \in n} \beta_j f_j^n(\mathbf{r}') \quad \mathbf{r} \in \Omega_1. \quad (53)$$

To check the BEM formulation against the above analytical example, the electron wave function is computed by setting the energy E in (11) to be one of the values (47). The contour plots of the wave functions relative to the first four energy levels, i.e., $E_{11}^{(\infty)}$, $E_{21}^{(\infty)}$, $E_{31}^{(\infty)}$ and $E_{12}^{(\infty)}$, are displayed in Figure 4 and can be shown to match those of the analytic solutions (46), not reported here for brevity. Table 2 details the error \mathcal{E} in the reconstructed wave functions, expressed by the following integral:

$$\mathcal{E} \equiv \sqrt{\int_{\Omega_1} d\mathbf{r} \left| \psi_1^{(\infty)}(\mathbf{r}) - \psi_1(\mathbf{r}) \right|^2} \quad (54)$$

In Figure 5, formula (54) is evaluated for an increasing number of mesh elements to check the convergence of the BEM algorithm. As illustrated in Figure 6, a further validation to the model is provided by comparing (47) with the energy values that lead to a local minimum of the function $|\det \mathbf{s}_1(E)|$, where \mathbf{s}_1 is the matrix defined in (52).

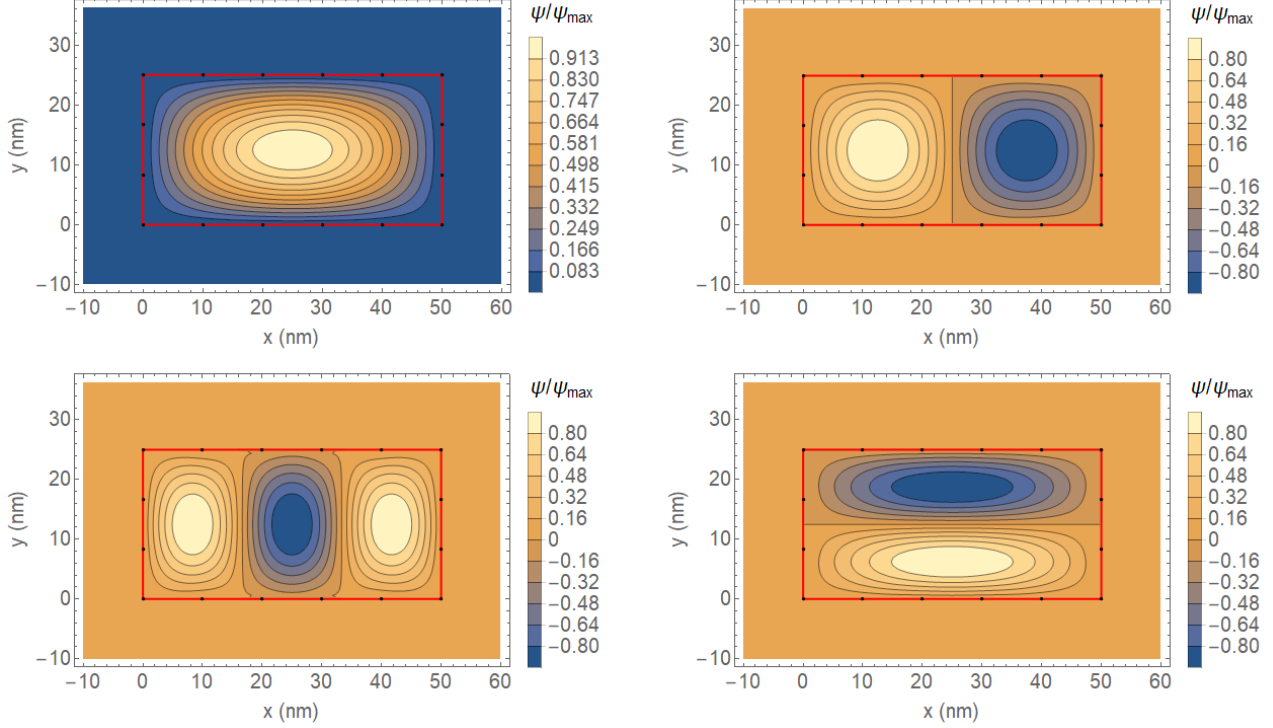


Figure 4. Contour plots of the first four bound electron wave functions in a rectangular structure of size $50 \times 25 \text{ nm}^2$ with $m_1 = m_2 = 0.0665 m_e$ and $V \gg E$. The wave functions are computed by the proposed BEM formulation via (51) and (53) using a mesh of 16 elements, first-order basis functions and a 10 points Gauss-Legendre quadrature for the numerical integrations.

n_x	1	2	3	1
n_y	1	1	1	2
\mathcal{E}	0.01	0.02	0.04	0.03

Table 2. Numeric error (54) of the BEM in the approximation of the wave functions (46) inside a rectangular structure with the same parameters as in Figure 4.

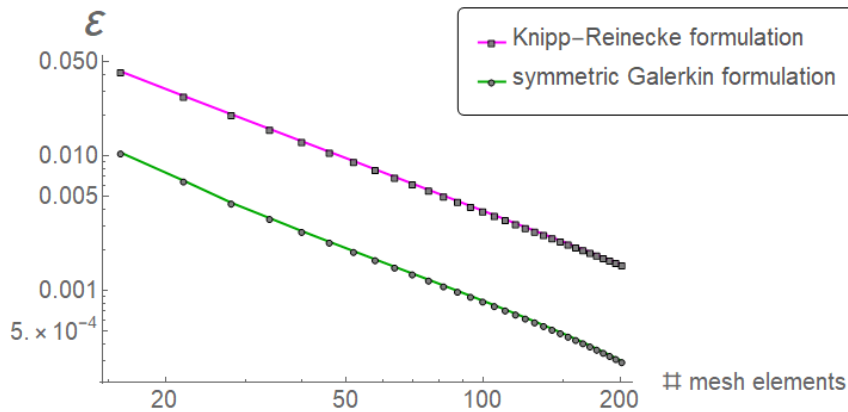


Figure 5. BEM error in the approximation of the first bound electron state inside a rectangular structure as a function of the number of mesh elements for the same choice of parameters adopted in Figure 4. The proposed symmetric Galerkin formulation is compared with that in [5].

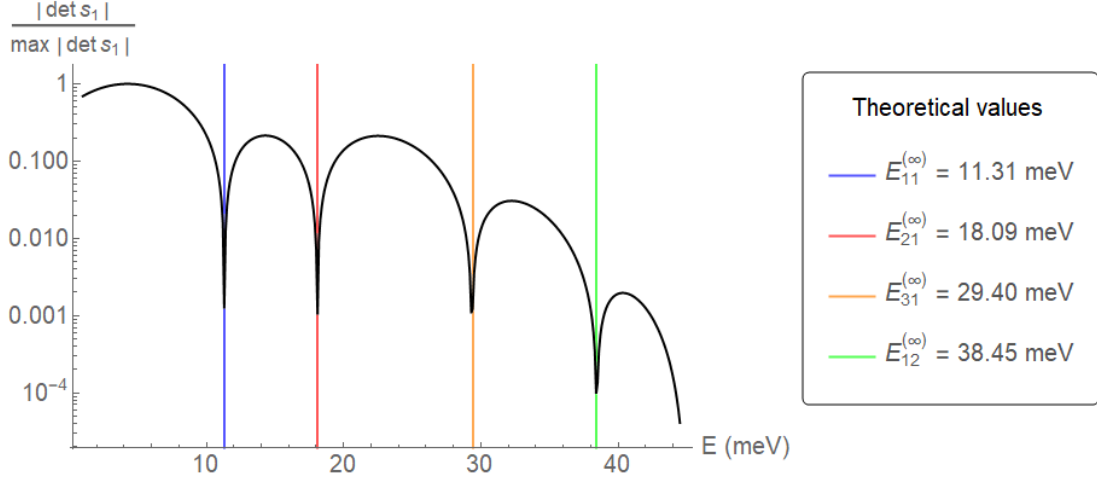


Figure 6. Determinant of the matrix (52) as a function of the electron energy for the same choice of parameters adopted in Figure 4.

4. Scattering states

4.1. Integral equations

Considering again the arbitrary two-region system introduced in Section 3, let us assume:

$$V(\mathbf{r}) = \begin{cases} V & \mathbf{r} \in \Omega_1; \\ 0 & \mathbf{r} \in \Omega_2, \end{cases} \quad m(\mathbf{r}) = \begin{cases} m_1 & \mathbf{r} \in \Omega_1; \\ m_2 & \mathbf{r} \in \Omega_2, \end{cases} \quad (55)$$

so that the wavenumbers in (10) are given by:

$$k_1^2 = \frac{2m_1}{\hbar^2} (E - V), \quad k_2^2 = \frac{2m_2}{\hbar^2} E. \quad (56)$$

We then express $\psi(\mathbf{r})$ as the superposition of a known incident wave function $\psi_{\text{inc}}(\mathbf{r})$ with energy E and an additional wave function $\Phi(\mathbf{r})$ such that $\Phi(\mathbf{r}) \rightarrow 0$ for large \mathbf{r} :

$$\psi(\mathbf{r}) = \begin{cases} \psi_1(\mathbf{r}) \equiv \Phi_1(\mathbf{r}) & \mathbf{r} \in \Omega_1; \\ \psi_2(\mathbf{r}) \equiv \psi_{\text{inc}}(\mathbf{r}) + \Phi_2(\mathbf{r}) & \mathbf{r} \in \Omega_2. \end{cases} \quad (57)$$

Under these assumptions, (10) becomes:

$$\Delta\Phi_j(\mathbf{r}) + k_j^2\Phi_j(\mathbf{r}) = 0 \quad j = 1, 2. \quad (58)$$

Combining this equation with (14) and repeating the procedure of Section 3.1, we obtain:

$$\begin{cases} \Phi_1(\mathbf{r}) = \int_S d\mathbf{r}' \left[g_1 \frac{\partial\Phi_1(\mathbf{r}')}{\partial n'} - \Phi_1(\mathbf{r}') \frac{\partial g_1}{\partial n'} \right] & \mathbf{r} \in \Omega_1; \\ \Phi_2(\mathbf{r}) = \int_S d\mathbf{r}' \left[\Phi_2(\mathbf{r}') \frac{\partial g_2}{\partial n'} - g_2 \frac{\partial\Phi_2(\mathbf{r}')}{\partial n'} \right] & \mathbf{r} \in \Omega_2. \end{cases} \quad (59)$$

Furthermore, by carefully taking the limit to the boundary:

$$\begin{cases} \frac{\Phi_1(\mathbf{r})}{2} = \int_S d\mathbf{r}' \left[g_1 \frac{\partial\Phi_1(\mathbf{r}')}{\partial n'} - \Phi_1(\mathbf{r}') \frac{\partial g_1}{\partial n'} \right] & \mathbf{r} \in S; \\ \frac{\Phi_2(\mathbf{r})}{2} = \int_S d\mathbf{r}' \left[\Phi_2(\mathbf{r}') \frac{\partial g_2}{\partial n'} - g_2 \frac{\partial\Phi_2(\mathbf{r}')}{\partial n'} \right] & \mathbf{r} \in S. \end{cases} \quad (60)$$

Let now:

$$\Upsilon_j(\mathbf{r}_S) \equiv \frac{1}{m_j} \frac{\partial \psi_j(\mathbf{r}_S)}{\partial n}, \quad \chi_j(\mathbf{r}_S) \equiv \frac{1}{m_j} \frac{\partial \Phi_j(\mathbf{r}_S)}{\partial n} \quad j = 1, 2. \quad (61)$$

With this conventions, and taking into account (20), the boundary conditions read:

$$\begin{cases} \delta\psi(\mathbf{r}_S) \equiv \psi_2(\mathbf{r}_S) - \psi_1(\mathbf{r}_S) = 0 & \Rightarrow \psi_2(\mathbf{r}_S) = \psi_1(\mathbf{r}_S) = \Phi_1(\mathbf{r}_S); \\ \delta\Upsilon(\mathbf{r}_S) \equiv \Upsilon_2(\mathbf{r}_S) - \Upsilon_1(\mathbf{r}_S) = 0 & \Rightarrow \Upsilon_2(\mathbf{r}_S) = \Upsilon_1(\mathbf{r}_S) = \chi_1(\mathbf{r}_S), \end{cases} \quad (62)$$

therefore:

$$\Phi_2(\mathbf{r}_S) = \Phi_1(\mathbf{r}_S) - \psi_{\text{inc}}(\mathbf{r}_S), \quad \chi_2(\mathbf{r}_S) = \chi_1(\mathbf{r}_S) - \frac{1}{m_2} \frac{\partial \psi_{\text{inc}}(\mathbf{r}_S)}{\partial n}. \quad (63)$$

By redefining $\Phi_1(\mathbf{r}_S) \equiv \Phi(\mathbf{r}_S)$ and $\chi_1(\mathbf{r}_S) \equiv \chi(\mathbf{r}_S)$, the first equation in system (60) is easily recast into the form:

$$\oint_S d\mathbf{r}'_S \left[\frac{\partial g_1(\mathbf{r}_S, \mathbf{r}'_S)}{\partial n'} \Phi(\mathbf{r}'_S) - m_1 g_1(\mathbf{r}_S, \mathbf{r}'_S) \chi(\mathbf{r}'_S) \right] = -\frac{\Phi(\mathbf{r}_S)}{2}. \quad (64)$$

We now combine the Helmholtz equation for $\psi_{\text{inc}}(\mathbf{r})$ with (14) to get:

$$g_2(\mathbf{r}, \mathbf{r}') \Delta' \psi_{\text{inc}}(\mathbf{r}') - \psi_{\text{inc}}(\mathbf{r}') \Delta' g_2(\mathbf{r}, \mathbf{r}') = \psi_{\text{inc}}(\mathbf{r}') \delta(\mathbf{r} - \mathbf{r}'). \quad (65)$$

For $\mathbf{r} \in \Omega_2$, the integral of the above expression over Ω_1 can be rewritten using (16):

$$\int_S d\mathbf{r}'_S \left[g_2(\mathbf{r}, \mathbf{r}'_S) \frac{\partial \psi_{\text{inc}}(\mathbf{r}'_S)}{\partial n'} - \frac{\partial g_2(\mathbf{r}, \mathbf{r}'_S)}{\partial n'} \psi_{\text{inc}}(\mathbf{r}'_S) \right] = 0 \quad \mathbf{r} \in \Omega_2. \quad (66)$$

Taking with due care the limit $\mathbf{r} \rightarrow \mathbf{r}_S$, we obtain:

$$\oint_S d\mathbf{r}'_S \left[\frac{\partial g_2(\mathbf{r}_S, \mathbf{r}'_S)}{\partial n'} \psi_{\text{inc}}(\mathbf{r}'_S) - g_2(\mathbf{r}_S, \mathbf{r}'_S) \frac{\partial \psi_{\text{inc}}(\mathbf{r}'_S)}{\partial n'} \right] = -\frac{\psi_{\text{inc}}(\mathbf{r}_S)}{2} \quad (67)$$

Then, considering the second equation in (60):

$$\oint_S d\mathbf{r}'_S \left[\frac{\partial g_2(\mathbf{r}_S, \mathbf{r}'_S)}{\partial n'} \Phi_2(\mathbf{r}'_S) - g_2(\mathbf{r}_S, \mathbf{r}'_S) \frac{\partial \Phi_2(\mathbf{r}'_S)}{\partial n'} \right] = \frac{\Phi_2(\mathbf{r}_S)}{2} \quad (68)$$

and summing the last two expressions, with reference to (57) and (61), leads to:

$$\oint_S d\mathbf{r}'_S \left[\frac{\partial g_2(\mathbf{r}_S, \mathbf{r}'_S)}{\partial n'} \psi_2(\mathbf{r}'_S) - m_2 g_2(\mathbf{r}_S, \mathbf{r}'_S) \Upsilon_2(\mathbf{r}'_S) \right] = \frac{\psi_2(\mathbf{r}_S)}{2} - \psi_{\text{inc}}(\mathbf{r}_S) \quad (69)$$

If we resort to (62), $\Phi_1(\mathbf{r}_S) \equiv \Phi(\mathbf{r}_S)$ and $\chi_1(\mathbf{r}_S) \equiv \chi(\mathbf{r}_S)$, the previous equation becomes:

$$\oint_S d\mathbf{r}'_S \left[\frac{\partial g_2(\mathbf{r}_S, \mathbf{r}'_S)}{\partial n'} \Phi(\mathbf{r}'_S) - m_2 g_2(\mathbf{r}_S, \mathbf{r}'_S) \chi(\mathbf{r}'_S) \right] = \frac{\Phi(\mathbf{r}_S)}{2} - \psi_{\text{inc}}(\mathbf{r}_S). \quad (70)$$

Finally, the sum of (70) and (64) gives:

$$\oint_S d\mathbf{r}'_S \left[\frac{\partial g_1(\mathbf{r}_S, \mathbf{r}'_S)}{\partial n'} + \frac{\partial g_2(\mathbf{r}_S, \mathbf{r}'_S)}{\partial n'} \right] \Phi(\mathbf{r}'_S) - \oint_S d\mathbf{r}'_S [m_1 g_1(\mathbf{r}_S, \mathbf{r}'_S) + m_2 g_2(\mathbf{r}_S, \mathbf{r}'_S)] \chi(\mathbf{r}'_S) = -\psi_{\text{inc}}(\mathbf{r}_S) \quad (71)$$

which constitutes the first integral equation of the BEM system.

In order to arrive at the second equation, we first need to consider (26) and compute the normal derivative of (59) at S_ε^\mp , respectively:

$$\begin{cases} \frac{\partial \Phi_1(\mathbf{r})}{\partial n_-} = \int_S d\mathbf{r}' \left[\frac{\partial g_1}{\partial n_-} \frac{\partial \Phi_1(\mathbf{r}')}{\partial n'} - \Phi_1(\mathbf{r}') \frac{\partial^2 g_1}{\partial n_- \partial n'} \right] & \mathbf{r} \in S_\varepsilon^-; \\ \frac{\partial \Phi_2(\mathbf{r})}{\partial n_+} = \int_S d\mathbf{r}' \left[\Phi_2(\mathbf{r}') \frac{\partial^2 g_2}{\partial n_+ \partial n'} - \frac{\partial g_2}{\partial n_+} \frac{\partial \Phi_2(\mathbf{r}')}{\partial n'} \right] & \mathbf{r} \in S_\varepsilon^+. \end{cases} \quad (72)$$

We also evaluate the normal derivative of (66) at S_ε^+ :

$$\int_S d\mathbf{r}'_S \left[\frac{\partial^2 g_2(\mathbf{r}, \mathbf{r}'_S)}{\partial n_+ \partial n'} \psi_{\text{inc}}(\mathbf{r}'_S) - \frac{\partial g_2(\mathbf{r}, \mathbf{r}'_S)}{\partial n_+} \frac{\partial \psi_{\text{inc}}(\mathbf{r}'_S)}{\partial n'} \right] = 0 \quad \mathbf{r} \in S_\varepsilon^+. \quad (73)$$

Then, taking the second equation in (72):

$$\int_S d\mathbf{r}'_S \left[\frac{\partial^2 g_2(\mathbf{r}, \mathbf{r}'_S)}{\partial n_+ \partial n'} \Phi_2(\mathbf{r}'_S) - \frac{\partial g_2(\mathbf{r}, \mathbf{r}'_S)}{\partial n_+} \frac{\partial \Phi_2(\mathbf{r}'_S)}{\partial n'} \right] = \frac{\partial \Phi_2(\mathbf{r})}{\partial n_+} \quad \mathbf{r} \in S_\varepsilon^+ \quad (74)$$

and combining it with the above expression, we obtain:

$$\frac{\partial \psi_2(\mathbf{r})}{\partial n_+} = \frac{\partial \psi_{\text{inc}}(\mathbf{r})}{\partial n_+} + \int_S d\mathbf{r}'_S \left[\frac{\partial^2 g_2(\mathbf{r}, \mathbf{r}'_S)}{\partial n_+ \partial n'} \psi_2(\mathbf{r}'_S) - m_2 \frac{\partial g_2(\mathbf{r}, \mathbf{r}'_S)}{\partial n_+} \gamma_2(\mathbf{r}'_S) \right] \quad \mathbf{r} \in S_\varepsilon^+. \quad (75)$$

On the other hand, we still have the first equation in (72):

$$\frac{\partial \Phi_1(\mathbf{r})}{\partial n_-} = \int_S d\mathbf{r}'_S \left[\frac{\partial g_1(\mathbf{r}, \mathbf{r}'_S)}{\partial n_-} \frac{\partial \Phi_1(\mathbf{r}'_S)}{\partial n'} - \Phi_1(\mathbf{r}'_S) \frac{\partial^2 g_1(\mathbf{r}, \mathbf{r}'_S)}{\partial n_- \partial n'} \right] \quad \mathbf{r} \in S_\varepsilon^-. \quad (76)$$

Dividing (75) by m_2 , (76) by m_1 and taking the difference between the two under the limit $\varepsilon \rightarrow 0$ gives:

$$\begin{aligned} & \int_S d\mathbf{r}'_S \left[\frac{1}{m_1} \frac{\partial^2 g_1(\mathbf{r}_S, \mathbf{r}'_S)}{\partial n \partial n'} + \frac{1}{m_2} \frac{\partial^2 g_2(\mathbf{r}_S, \mathbf{r}'_S)}{\partial n \partial n'} \right] \Phi(\mathbf{r}'_S) - \int_S d\mathbf{r}'_S \left[\frac{\partial g_1(\mathbf{r}_S, \mathbf{r}'_S)}{\partial n} + \frac{\partial g_2(\mathbf{r}_S, \mathbf{r}'_S)}{\partial n} \right] \chi(\mathbf{r}'_S) \\ &= -\frac{1}{m_2} \frac{\partial \psi_{\text{inc}}(\mathbf{r}_S)}{\partial n}, \end{aligned} \quad (77)$$

which then completes our BEM system. Proceeding as in Section 3.1, equations (71) and (77) can be expressed in matrix form:

$$\hat{\mathbf{H}} \begin{bmatrix} \Phi \\ \chi \end{bmatrix}(\mathbf{r}_S) = \mathbf{J}(\mathbf{r}_S), \quad (78)$$

where $\hat{\mathbf{H}}$ is the matrix integral operator defined in (30) and:

$$\mathbf{J}(\mathbf{r}_S) \equiv \begin{pmatrix} \psi_{\text{inc}}(\mathbf{r}_S) \\ \frac{1}{m_2} \frac{\partial \psi_{\text{inc}}(\mathbf{r}_S)}{\partial n} \end{pmatrix}. \quad (79)$$

Summarizing, the electron wave function in the two regions has been rewritten through (57) in terms of a known incident wave function $\psi_{\text{inc}}(\mathbf{r})$ and a scattered field $\Phi(\mathbf{r})$ which satisfies:

$$\begin{cases} \Phi_1(\mathbf{r}) = \int_S d\mathbf{r}'_S \left[m_1 g_1(\mathbf{r}, \mathbf{r}'_S) \chi(\mathbf{r}'_S) - \frac{\partial g_1(\mathbf{r}, \mathbf{r}'_S)}{\partial n'} \Phi(\mathbf{r}'_S) \right] & \mathbf{r} \in \Omega_1; \\ \Phi_2(\mathbf{r}) = \int_S d\mathbf{r}'_S \left[\frac{\partial g_2(\mathbf{r}, \mathbf{r}'_S)}{\partial n'} \Phi(\mathbf{r}'_S) - m_2 g_2(\mathbf{r}, \mathbf{r}'_S) \chi(\mathbf{r}'_S) \right] & \mathbf{r} \in \Omega_2, \end{cases} \quad (80)$$

with $\Phi(\mathbf{r}_S)$ and $\chi(\mathbf{r}_S)$ representing the solution of the matrix integral equation (78). Contrary to [5], the proposed formulation results in a very concise form of the inhomogeneous term $\mathbf{J}(\mathbf{r}_S)$, dictated only by the boundary restrictions of the incident wave function and its normal derivative.

4.2. Scattering amplitude

When the incident wave function $\psi_{\text{inc}}(\mathbf{r})$ is taken to be a plane wave $\exp(i\mathbf{k}_{\text{inc}} \cdot \mathbf{r})$ with $|\mathbf{k}_{\text{inc}}| = k_2$, in the outer region at great distances from the boundary S we have:

$$\psi_2(\mathbf{r}) \sim \exp(i\mathbf{k}_{\text{inc}} \cdot \mathbf{r}) + g_2(\mathbf{r}, 0) F(\mathbf{k}), \quad (81)$$

where $\mathbf{k} \equiv k_2 \hat{\mathbf{r}}$,

$$g_2(\mathbf{r}, 0) \sim \begin{cases} \frac{i}{4} \sqrt{\frac{2}{\pi k_2 r}} \exp(ik_2 r - i\frac{\pi}{4}) & \text{2D;} \\ \frac{1}{4\pi r} \exp(ik_2 r) & \text{3D} \end{cases} \quad (82)$$

and:

$$F(\mathbf{k}) \equiv \begin{cases} 2\sqrt{\pi k_2} (1-i) f^{(2\text{D})}(\mathbf{k}) & \text{2D;} \\ 4\pi f^{(3\text{D})}(\mathbf{k}) & \text{3D,} \end{cases} \quad (83)$$

being $f^{(2\text{D})}(\mathbf{k})$ and $f^{(3\text{D})}(\mathbf{k})$ the differential scattering amplitudes in two and three dimensions, respectively. Now, combining the second equation in (59) with (66) for $\mathbf{r} \gg \mathbf{r}'_S$ and making use of the far-field approximation:

$$k_2 |\mathbf{r} - \mathbf{r}'_S| \sim k_2 \left(r - \frac{\mathbf{r} \cdot \mathbf{r}'_S}{r} \right) = k_2 r - \mathbf{k} \cdot \mathbf{r}'_S, \quad (84)$$

we can write:

$$\psi_2(\mathbf{r}) \sim \exp(i\mathbf{k}_{\text{inc}} \cdot \mathbf{r}) - g_2(\mathbf{r}, 0) \int_S d\mathbf{r}'_S [i\mathbf{k} \cdot \mathbf{n}' \Phi(\mathbf{r}'_S) + m_2 \chi(\mathbf{r}'_S)] \exp(-i\mathbf{k} \cdot \mathbf{r}'_S). \quad (85)$$

From the comparison between (81) and (85), it follows that:

$$F(\mathbf{k}) = - \int_S d\mathbf{r}'_S [i\mathbf{k} \cdot \mathbf{n}' \Phi(\mathbf{r}'_S) + m_2 \chi(\mathbf{r}'_S)] \exp(-i\mathbf{k} \cdot \mathbf{r}'_S). \quad (86)$$

4.3. Discretization of the operators

The integral equations so far derived can be discretized just as in Section 3.2, after expanding the boundary restrictions of the scattered field and of its inverse mass weighted normal derivative on a set of node-based basis functions:

$$\Phi(\mathbf{r}'_S) = \sum_j \alpha_j f_j(\mathbf{r}'_S); \quad \chi(\mathbf{r}'_S) = \mu^{-1} \sum_j \beta_j f_j(\mathbf{r}'_S). \quad (87)$$

This results in the following Galerkin-discretized version of system (78):

$$\sum_j \mathbf{H}_{ij} \begin{bmatrix} \alpha_j \\ \beta_j \end{bmatrix} = \mathbf{J}_i, \quad (88)$$

where \mathbf{H}_{ij} is defined in (39) and:

$$\mathbf{J}_i \equiv \sum_{m \in i} \int_{S_m} d\mathbf{r} \left(\frac{\psi_{\text{inc}}(\mathbf{r})}{m_2} \frac{\partial \psi_{\text{inc}}(\mathbf{r})}{\partial n} \right) f_i^m(\mathbf{r}). \quad (89)$$

A numerical solution to (88) is then achieved by matrix inversion³:

$$\begin{bmatrix} \alpha_i \\ \beta_i \end{bmatrix} = \sum_j \mathbf{H}_{ij}^{-1} \mathbf{J}_j \quad (90)$$

³ See also Appendix E.

and makes it possible to determine the BEM wave function from (80):

$$\begin{cases} \Phi_1(\mathbf{r}) = \sum_n \int_{S_n} d\mathbf{r}' \sum_{j \in n} \left[\beta_j \frac{m_1}{\mu} g_1(\mathbf{r}, \mathbf{r}') - \alpha_j \frac{\partial g_1(\mathbf{r}, \mathbf{r}')}{\partial n'} \right] f_j^n(\mathbf{r}') & \mathbf{r} \in \Omega_1; \\ \Phi_2(\mathbf{r}) = \sum_n \int_{S_n} d\mathbf{r}' \sum_{j \in n} \left[\alpha_j \frac{\partial g_2(\mathbf{r}, \mathbf{r}')}{\partial n'} - \beta_j \frac{m_2}{\mu} g_2(\mathbf{r}, \mathbf{r}') \right] f_j^n(\mathbf{r}') & \mathbf{r} \in \Omega_2, \end{cases} \quad (91)$$

as well as the BEM scattering amplitude from (86):

$$F(\mathbf{k}) = - \sum_n \int_{S_n} d\mathbf{r}' \sum_{j \in n} \left[i\alpha_j \mathbf{k} \cdot \mathbf{n}' + \beta_j \frac{m_2}{\mu} \right] f_j^n(\mathbf{r}') \exp(-i\mathbf{k} \cdot \mathbf{r}'). \quad (92)$$

4.4. Examples and comparisons

Assuming $\psi_{\text{inc}}(\mathbf{r}) = \exp(i\mathbf{k}_{\text{inc}} \cdot \mathbf{r})$ with:

$$\mathbf{k}_{\text{inc}} = k_2 \cos \theta_{\text{inc}} \hat{\mathbf{x}} + k_2 \sin \theta_{\text{inc}} \hat{\mathbf{y}}, \quad (93)$$

we now reintroduce the rectangle and stadium geometries considered in Section 3.3 and set the band offset V in (55) and the electron energy E to be 200 meV and 150 meV, respectively. Figure 7 displays the total electron wave function (57) in the two geometries for two different values of θ_{inc} . By choosing:

$$\mathbf{k} = k_2 \cos \theta \hat{\mathbf{x}} + k_2 \sin \theta \hat{\mathbf{y}}, \quad (94)$$

the differential scattering amplitude $f^{(2D)}(\mathbf{k})$ obtained from (83) and (92) can be rewritten as a function of the angle θ and the total scattering cross section is defined as:

$$\sigma \equiv \int_0^{2\pi} \left| f^{(2D)}(\theta) \right|^2 d\theta. \quad (95)$$

For the sake of comparison, both $\left| f^{(2D)}(\theta) \right|^2$ and σ are shown in Figure 8 for a rectangular quantum dot like that considered in [5]. As expected, the results match very well.

5. Spectral density function

5.1. Integral equations

Taking E_ν and $\psi^{(\nu)}(\mathbf{r})$ to represent the energy and normalized wave function of the ν -th quantum state of the electron, the spectral density function:

$$\rho(\mathbf{r}, \mathbf{r}'; E) \equiv \sum_\nu \frac{\psi^{(\nu)}(\mathbf{r}) \left[\psi^{(\nu)}(\mathbf{r}') \right]^*}{E_\nu - E} \quad (96)$$

provides a unified description of both the discrete and continuous portions of the spectrum [5]. Within the arbitrary two-region system so far considered, the spectral density function may be rewritten as:

$$\rho(\mathbf{r}, \mathbf{r}'; E) \equiv \begin{cases} \rho_1(\mathbf{r}, \mathbf{r}'; E) & \mathbf{r}, \mathbf{r}' \in \Omega_1; \\ \rho_2(\mathbf{r}, \mathbf{r}'; E) & \mathbf{r}, \mathbf{r}' \in \Omega_2 \end{cases} \quad (97)$$

and it is found to satisfy:

$$\Delta \rho_j(\mathbf{r}, \mathbf{r}'; E) + k_j^2 \rho_j(\mathbf{r}, \mathbf{r}'; E) = -\frac{2m_j}{\hbar^2} \delta(\mathbf{r} - \mathbf{r}') \quad j = 1, 2, \quad (98)$$

as follows from (13) and from the completeness relation:

$$\sum_\nu \psi^{(\nu)}(\mathbf{r}) \left[\psi^{(\nu)}(\mathbf{r}') \right]^* = \delta(\mathbf{r} - \mathbf{r}'). \quad (99)$$

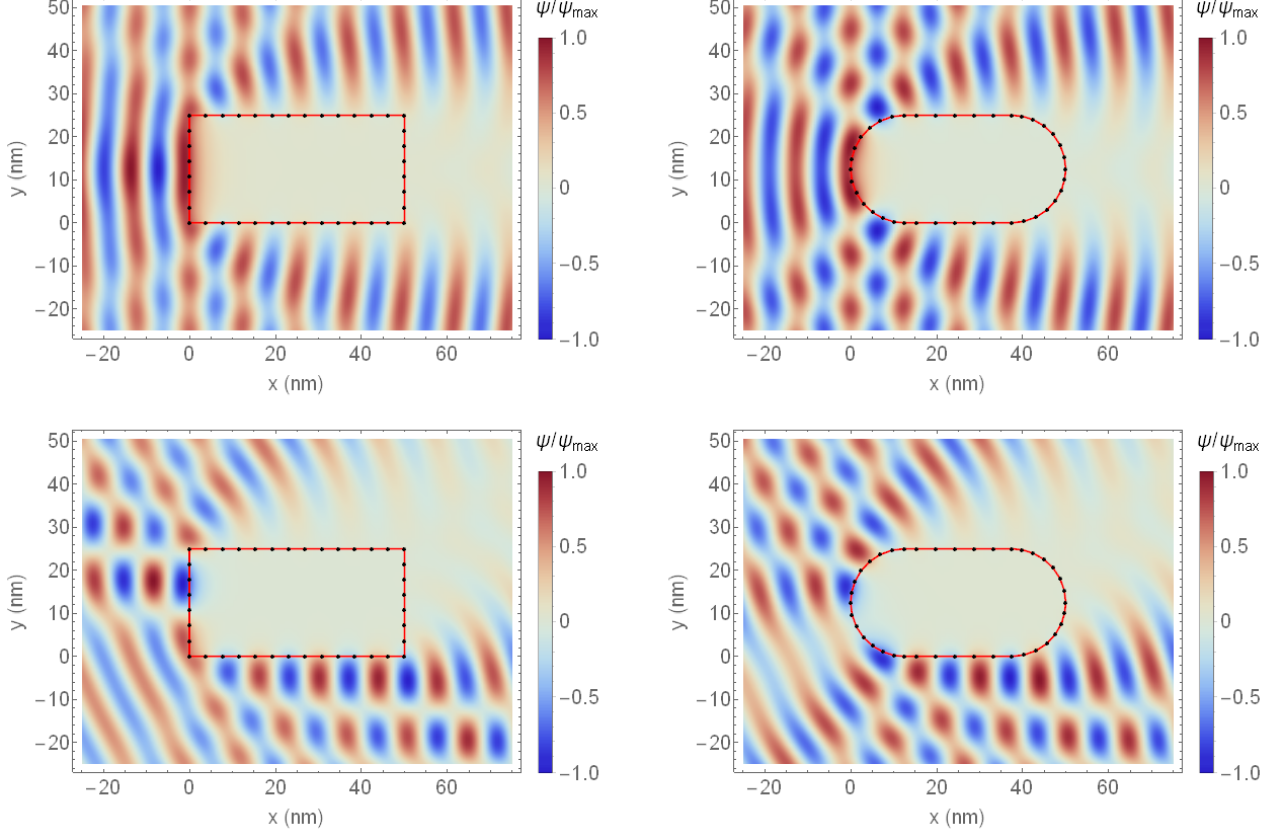


Figure 7. Scattering of an electron of energy $E = 150$ meV from a rectangular (*left*) and stadium-shaped (*right*) quantum dot of size 50×25 nm² with $m_1 = m_2 = 0.0665 m_e$ and $V = 200$ meV. The total wave function is computed by the proposed BEM formulation via (88) and (91) for an electron impinging with $\theta_{\text{inc}} = 0$ (*top*) and with $\theta_{\text{inc}} = \arctan(L_y/L_x)$ (*bottom*), using a mesh of 40 elements, first-order basis functions and a 10 points Gauss-Legendre quadrature for the numerical integrations.

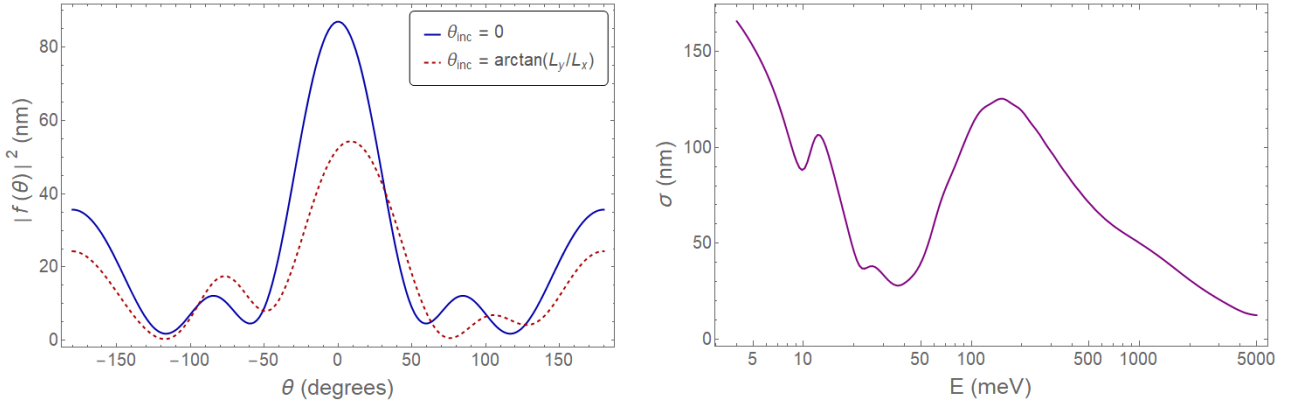


Figure 8. Scattering of an electron that moves along the x -axis from a rectangular quantum dot of size 48×24 nm² with $m_1 = m_2 = 0.0665 m_e$ and $V = -50$ meV. *Left*: differential scattering cross section with respect to the θ angle for $E = 5$ meV. *Right*: total scattering cross section (95) as a function of the electron energy. Both results are obtained by the proposed BEM formulation via (88) and (92) using a mesh of 40 elements, first-order basis functions and a 10 points Gauss-Legendre quadrature for the numerical integrations.

Furthermore, by introducing:

$$\Pi_j(\mathbf{r}_S, \mathbf{r}'_S; E) \equiv \frac{1}{m_j} \frac{\partial \rho_j(\mathbf{r}_S, \mathbf{r}'_S; E)}{\partial n} \quad j = 1, 2, \quad (100)$$

from (23) we have:

$$\begin{cases} \rho_2(\mathbf{r}_S, \mathbf{r}'_S; E) = \rho_1(\mathbf{r}_S, \mathbf{r}'_S; E) \equiv \rho(\mathbf{r}_S, \mathbf{r}'_S; E); \\ \Pi_2(\mathbf{r}_S, \mathbf{r}'_S; E) = \Pi_1(\mathbf{r}_S, \mathbf{r}'_S; E) \equiv \Pi(\mathbf{r}_S, \mathbf{r}'_S; E); \end{cases} \quad (101)$$

Equations (14) and (98) can be easily manipulated and combined to obtain:

$$g_j(\mathbf{r}, \mathbf{r}') \Delta' \rho_j(\mathbf{r}', \mathbf{r}'') - \rho_j(\mathbf{r}', \mathbf{r}'') \Delta' g_j(\mathbf{r}, \mathbf{r}') = \rho_j(\mathbf{r}', \mathbf{r}'') \delta(\mathbf{r} - \mathbf{r}') - \frac{2m_j}{\hbar^2} g_j(\mathbf{r}, \mathbf{r}') \delta(\mathbf{r}' - \mathbf{r}'') \quad j = 1, 2, \quad (102)$$

where $\mathbf{r}, \mathbf{r}', \mathbf{r}'' \in \Omega_j$ and the energy dependence of the spectral density function has been suppressed for brevity. Integrating the expression in $d\mathbf{r}'$ over the volume $\Omega_j \setminus B_\varrho(\mathbf{r})$ and using (16), we get:

$$\int_S d\mathbf{r}'_S \left[g_1(\mathbf{r}, \mathbf{r}'_S) \frac{\partial \rho_1(\mathbf{r}'_S, \mathbf{r}'')}{\partial n'} - \rho_1(\mathbf{r}'_S, \mathbf{r}'') \frac{\partial g_1(\mathbf{r}, \mathbf{r}'_S)}{\partial n'} \right] = \rho_1(\mathbf{r}, \mathbf{r}'') - \frac{2m_1}{\hbar^2} g_1(\mathbf{r}, \mathbf{r}'') \quad (103)$$

for $\mathbf{r}, \mathbf{r}'' \in \Omega_1$, and:

$$\int_S d\mathbf{r}'_S \left[\rho_2(\mathbf{r}'_S, \mathbf{r}'') \frac{\partial g_2(\mathbf{r}, \mathbf{r}'_S)}{\partial n'} - g_2(\mathbf{r}, \mathbf{r}'_S) \frac{\partial \rho_2(\mathbf{r}'_S, \mathbf{r}'')}{\partial n'} \right] = \rho_2(\mathbf{r}, \mathbf{r}'') - \frac{2m_2}{\hbar^2} g_2(\mathbf{r}, \mathbf{r}'') \quad (104)$$

for $\mathbf{r}, \mathbf{r}'' \in \Omega_2$. Under the limits $\mathbf{r} \rightarrow \mathbf{r}_S$ and $\mathbf{r}'' \rightarrow \mathbf{r}''_S$, (103) and (104) reduce to:

$$\oint_S d\mathbf{r}'_S \left[g_1(\mathbf{r}_S, \mathbf{r}'_S) \frac{\partial \rho_1(\mathbf{r}'_S, \mathbf{r}''_S)}{\partial n'} - \rho_1(\mathbf{r}'_S, \mathbf{r}''_S) \frac{\partial g_1(\mathbf{r}_S, \mathbf{r}'_S)}{\partial n'} \right] = \frac{\rho_1(\mathbf{r}_S, \mathbf{r}''_S)}{2} - \frac{m_1}{\hbar^2} g_1(\mathbf{r}_S, \mathbf{r}''_S) \quad (105)$$

and:

$$\oint_S d\mathbf{r}'_S \left[\rho_2(\mathbf{r}'_S, \mathbf{r}''_S) \frac{\partial g_2(\mathbf{r}_S, \mathbf{r}'_S)}{\partial n'} - g_2(\mathbf{r}_S, \mathbf{r}'_S) \frac{\partial \rho_2(\mathbf{r}'_S, \mathbf{r}''_S)}{\partial n'} \right] = \frac{\rho_2(\mathbf{r}_S, \mathbf{r}''_S)}{2} - \frac{m_2}{\hbar^2} g_2(\mathbf{r}_S, \mathbf{r}''_S), \quad (106)$$

respectively. Taking the difference between the two resulting expressions with reference to (101), we arrive at:

$$\begin{aligned} & \oint_S d\mathbf{r}'_S \left[\frac{\partial g_1(\mathbf{r}_S, \mathbf{r}'_S)}{\partial n'} + \frac{\partial g_2(\mathbf{r}_S, \mathbf{r}'_S)}{\partial n'} \right] \rho(\mathbf{r}'_S, \mathbf{r}''_S) - \oint_S d\mathbf{r}'_S [m_1 g_1(\mathbf{r}_S, \mathbf{r}'_S) + m_2 g_2(\mathbf{r}_S, \mathbf{r}'_S)] \Pi(\mathbf{r}'_S, \mathbf{r}''_S) \\ & = \frac{m_1}{\hbar^2} g_1(\mathbf{r}_S, \mathbf{r}''_S) - \frac{m_2}{\hbar^2} g_2(\mathbf{r}_S, \mathbf{r}''_S). \end{aligned} \quad (107)$$

As it is now customary, the second equation of the BEM system can be obtained by combining the inverse mass weighted normal derivatives of (103) and (104) at $\mathbf{r} \in S_\varepsilon^\mp$ under the limit $\varepsilon \rightarrow 0$, which leads to:

$$\begin{aligned} & \int_S d\mathbf{r}'_S \left[\frac{1}{m_1} \frac{\partial^2 g_1(\mathbf{r}_S, \mathbf{r}'_S)}{\partial n \partial n'} + \frac{1}{m_2} \frac{\partial^2 g_2(\mathbf{r}_S, \mathbf{r}'_S)}{\partial n \partial n'} \right] \rho(\mathbf{r}'_S, \mathbf{r}''_S) - \oint_S d\mathbf{r}'_S \left[\frac{\partial g_1(\mathbf{r}_S, \mathbf{r}'_S)}{\partial n} + \frac{\partial g_2(\mathbf{r}_S, \mathbf{r}'_S)}{\partial n} \right] \\ & \times \Pi(\mathbf{r}'_S, \mathbf{r}''_S) = \frac{1}{\hbar^2} \left[\frac{\partial g_1(\mathbf{r}_S, \mathbf{r}''_S)}{\partial n} - \frac{\partial g_2(\mathbf{r}_S, \mathbf{r}''_S)}{\partial n} \right]. \end{aligned} \quad (108)$$

Equations (107) and (108) are rewritten compactly as:

$$\hat{\mathbf{H}} \begin{bmatrix} \rho \\ \Pi \end{bmatrix} (\mathbf{r}_S, \mathbf{r}''_S) = \mathbf{G}(\mathbf{r}_S, \mathbf{r}''_S), \quad (109)$$

where $\hat{\mathbf{H}}$ is still the same as in (30) and:

$$\mathbf{G}(\mathbf{r}_S, \mathbf{r}_S'') \equiv \frac{1}{\hbar^2} \begin{pmatrix} m_2 g_2(\mathbf{r}_S, \mathbf{r}_S'') - m_1 g_1(\mathbf{r}_S, \mathbf{r}_S'') \\ \frac{\partial g_2(\mathbf{r}_S, \mathbf{r}_S'')}{\partial n} - \frac{\partial g_1(\mathbf{r}_S, \mathbf{r}_S'')}{\partial n} \end{pmatrix}. \quad (110)$$

Finally, as suggested in [5], the boundary data can be condensed into the following distribution:

$$\rho_w(E) \equiv \int_S d\mathbf{r}_S \int_S d\mathbf{r}_S' w(\mathbf{r}_S, \mathbf{r}_S') \text{Im} [\rho(\mathbf{r}_S, \mathbf{r}_S'; E)], \quad (111)$$

being $w(\mathbf{r}_S, \mathbf{r}_S')$ an arbitrary weighting function.

5.2. Discretization of the operators

Since the boundary restrictions in (109) are now functions of two space variables besides the electron energy, their expansion on the set of node-based basis functions may be expressed as:

$$\rho(\mathbf{r}_S', \mathbf{r}_S''; E) = \sum_{j,k} \alpha_{jk}(E) f_j(\mathbf{r}_S') f_k(\mathbf{r}_S''); \quad \Pi(\mathbf{r}_S', \mathbf{r}_S''; E) = \mu^{-1} \sum_{j,k} \beta_{jk}(E) f_j(\mathbf{r}_S') f_k(\mathbf{r}_S''). \quad (112)$$

Multiplying equation (109) by $f_i(\mathbf{r}_S) f_l(\mathbf{r}_S'')$ and integrating twice over S using (37), we obtain:

$$\sum_{j,k} \mathbf{H}_{ij} \begin{bmatrix} \alpha_{jk} F_{kl} \\ \beta_{jk} F_{kl} \end{bmatrix} = \mathbf{G}_{il}, \quad (113)$$

where \mathbf{H}_{ij} is defined in (39),

$$F_{kl} \equiv \sum_{c \in k \wedge l} \int_{S_c} d\mathbf{r}'' f_k^c(\mathbf{r}'') f_l^c(\mathbf{r}'') \quad (114)$$

identifies a sparse symmetric matrix⁴ whose only non-vanishing entries are those for which the mesh nodes k and l belong to the same simplex S_c , and:

$$\mathbf{G}_{il} \equiv \frac{1}{\hbar^2} \sum_{m \in i} \sum_{p \in l} \int_{S_m} d\mathbf{r} \int_{S_p} d\mathbf{r}'' \begin{pmatrix} m_2 g_2(\mathbf{r}, \mathbf{r}'') - m_1 g_1(\mathbf{r}, \mathbf{r}'') \\ \mu \left[\frac{\partial g_2(\mathbf{r}, \mathbf{r}'')}{\partial n} - \frac{\partial g_1(\mathbf{r}, \mathbf{r}'')}{\partial n} \right] \end{pmatrix} f_i^m(\mathbf{r}) f_l^p(\mathbf{r}''). \quad (115)$$

From (111) and (112), it follows that:

$$\rho_w(E) = \sum_{m,n} \int_{S_m} d\mathbf{r} \int_{S_n} d\mathbf{r}' w(\mathbf{r}, \mathbf{r}') \sum_{i \in m} \sum_{j \in n} \text{Im} [\alpha_{ij}(E)] f_i^m(\mathbf{r}) f_j^n(\mathbf{r}'). \quad (116)$$

Taking the function $w(\mathbf{r}, \mathbf{r}')$ to be the Dirac delta $\delta(\mathbf{r} - \mathbf{r}')$, the previous expression becomes:

$$\rho_\delta(E) = \sum_{i,j} \text{Im} [\alpha_{ij}(E)] \sum_{c \in i \wedge j} \int_{S_c} d\mathbf{r} f_i^m(\mathbf{r}) f_j^m(\mathbf{r}) = \sum_{i,j} \text{Im} [\alpha_{ij}(E)] F_{ij}, \quad (117)$$

where the matrix F has already been defined in (114). Then, letting:

$$\begin{bmatrix} \tilde{\alpha}_{il} \\ \tilde{\beta}_{il} \end{bmatrix} \equiv \sum_k \begin{bmatrix} \alpha_{ik} F_{kl} \\ \beta_{ik} F_{kl} \end{bmatrix}, \quad (118)$$

⁴ For instance, in the two-dimensional case with first-order basis functions, it is easy to show that $F_{kl} = (L_1 + L_2)/3$ for $k = l$, $F_{kl} = L/6$ when the nodes k, l are first neighbors and $F_{kl} = 0$ otherwise, being L, L_1 and L_2 the sizes of the common segments S_c .

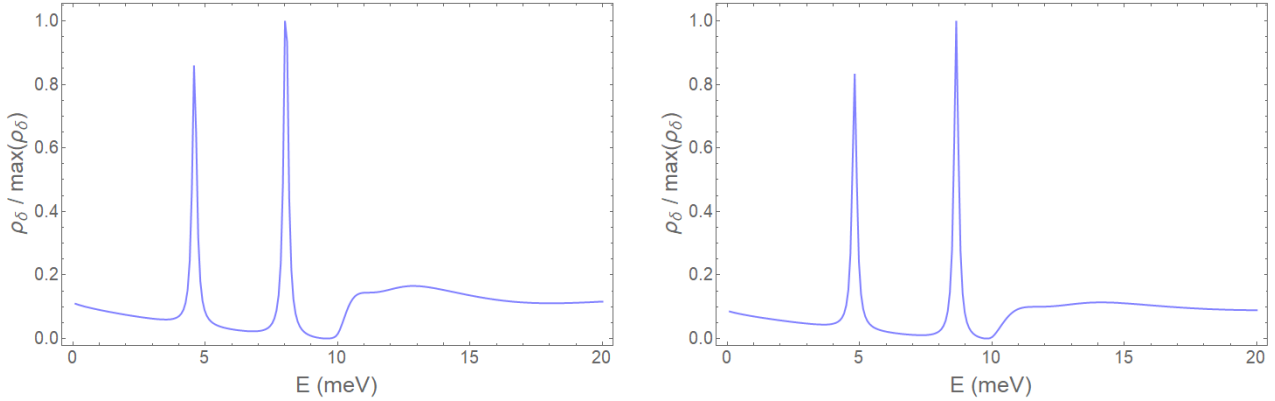


Figure 9. Spectral density of a rectangular (*left*) and stadium-shaped (*right*) structure of size $50 \times 25 \text{ nm}^2$ with $m_1 = m_2 = 0.0665 m_e$, $V = 10 \text{ meV}$ and $\text{Im}(E) = 0.1 \text{ meV}$. The spectral density function is computed by the proposed BEM formulation via (113), (118) and (120) using a mesh of 40 elements, first-order basis functions and a 10 points Gauss-Legendre quadrature for the numerical integrations.

equation (113) can be directly inverted⁵ to give:

$$\begin{bmatrix} \tilde{\alpha}_{il} \\ \tilde{\beta}_{il} \end{bmatrix} = \sum_j \mathbf{H}_{ij}^{-1} \mathbf{G}_{jl}. \quad (119)$$

It now becomes apparent that the knowledge of the matrix $\tilde{\alpha}$ enables us to easily determine the spectral density function from (117) and (118):

$$\rho_\delta(E) = \text{Im} \{ \text{tr} [\tilde{\alpha}(E)] \}. \quad (120)$$

The conciseness of this last result may be regarded as a further advantage of the proposed BEM formulation.

5.3. Examples and comparisons

The BEM-computed spectral density function $\rho_\delta(E)$ is reported in Figure 9 as a function of the electron energy for both the previously considered rectangle and stadium geometries. Since \mathbf{H} becomes singular when E approaches the bound portion of the spectrum, analytic continuation to complex energies may prove useful for display purposes, as explained in [5].

6. Conclusions

As the examples throughout the paper testify, the proposed symmetric Galerkin BEM gives very accurate results. Furthermore, it has the advantage of leading to a simple implementation of the inhomogeneous term in (88) and of the spectral density function in (120). It is worth noting that the integral equations (29), (78) and (109) can be generalized to systems composed of $N > 2$ subregions. Most importantly, owing to the spectral properties of the matrix integral operator (30), both (88) and (113) are suitable for preconditioning strategies based on the Calderon identities, as detailed in Appendix E. Despite direct inversion of the BEM matrix is not an issue for the academic problems analyzed so far, preconditioned iterative solvers may become essential to more realistic applications. The use of fast algorithms to speed up the proposed BEM formulation will be considered in future works.

⁵ See also Appendix E.

Acknowledgments

The authors wish to thank Prof. Francesco Andriulli for suggesting this study and two anonymous reviewers for their constructive comments which greatly improved the manuscript.

Appendix A. Proof of formula (18)

The free-space Green functions for the scalar Helmholtz equation in one, two and three dimensions are defined, respectively, as follows:

$$g^{(1D)}(x, x') \equiv \frac{i}{2k} \exp(ik|x - x'|); \quad (\text{A.1})$$

$$g^{(2D)}(\boldsymbol{\rho}, \boldsymbol{\rho}') \equiv \frac{i}{4} H_0^{(1)}(k|\boldsymbol{\rho} - \boldsymbol{\rho}'|); \quad (\text{A.2})$$

$$g^{(3D)}(\mathbf{r}, \mathbf{r}') \equiv \frac{\exp(ik|\mathbf{r} - \mathbf{r}'|)}{4\pi|\mathbf{r} - \mathbf{r}'|}. \quad (\text{A.3})$$

Let us write down the corresponding normal derivatives:

$$\frac{\partial g^{(1D)}(x, x')}{\partial n'} = \frac{1}{2} \exp(ik|x - x'|) \operatorname{sgn}(x - x') \frac{\partial x'}{\partial n'}; \quad (\text{A.4})$$

$$\frac{\partial g^{(2D)}(\boldsymbol{\rho}, \boldsymbol{\rho}')}{\partial n'} = \frac{ikH_1^{(1)}(k|\boldsymbol{\rho} - \boldsymbol{\rho}'|)}{4|\boldsymbol{\rho} - \boldsymbol{\rho}'|} (\boldsymbol{\rho} - \boldsymbol{\rho}') \cdot \mathbf{n}'; \quad (\text{A.5})$$

$$\frac{\partial g^{(3D)}(\mathbf{r}, \mathbf{r}')}{\partial n'} = -\frac{\exp(ik|\mathbf{r} - \mathbf{r}'|)}{4\pi|\mathbf{r} - \mathbf{r}'|^2} \left(ik - \frac{1}{|\mathbf{r} - \mathbf{r}'|} \right) (\mathbf{r} - \mathbf{r}') \cdot \mathbf{n}'. \quad (\text{A.6})$$

In the one-dimensional case, we have:

$$\begin{aligned} & \lim_{\varrho \rightarrow 0} \int_{\partial B_\varrho(\mathbf{r})} d\mathbf{r}' \left[g^{(1D)} \frac{\partial \psi(\mathbf{r}')}{\partial n'} - \psi(\mathbf{r}') \frac{\partial g^{(1D)}}{\partial n'} \right] \\ &= \lim_{\varrho \rightarrow 0} \left[g^{(1D)}(x, x + \varrho) \frac{\partial \psi(x + \varrho)}{\partial x} - g^{(1D)}(x, x - \varrho) \frac{\partial \psi(x - \varrho)}{\partial x} + \right. \\ & \quad \left. - \psi(x + \varrho) \frac{\partial g^{(1D)}(x, x + \varrho)}{\partial n'} - \psi(x - \varrho) \frac{\partial g^{(1D)}(x, x - \varrho)}{\partial n'} \right] \\ &= \lim_{\varrho \rightarrow 0} \left\{ \frac{i}{2k} \exp(ik\varrho) \left[\frac{\partial \psi(x + \varrho)}{\partial x} - \frac{\partial \psi(x - \varrho)}{\partial x} \right] + \frac{1}{2} \exp(ik\varrho) [\psi(x + \varrho) + \psi(x - \varrho)] \right\} = \psi(x). \end{aligned} \quad (\text{A.7})$$

Now, in two dimensions:

$$\begin{aligned} & \lim_{\varrho \rightarrow 0} \int_{\partial B_\varrho(\mathbf{r})} d\mathbf{r}' \left[g^{(2D)} \frac{\partial \psi(\mathbf{r}')}{\partial n'} - \psi(\mathbf{r}') \frac{\partial g^{(2D)}}{\partial n'} \right] \\ &= \lim_{\varrho \rightarrow 0} \int_0^{2\pi} d\varphi \varrho \left[\frac{i}{4} H_0^{(1)}(k\varrho) \frac{\partial \psi(\boldsymbol{\rho}')}{\partial n'} - \psi(\boldsymbol{\rho}') \frac{ikH_1^{(1)}(k\varrho)}{4\varrho} (\boldsymbol{\rho} - \boldsymbol{\rho}') \cdot \mathbf{n}' \right] \\ &= \lim_{\varrho \rightarrow 0} \int_0^{2\pi} d\varphi \varrho \left\{ \frac{i}{4} \frac{\partial \psi(\boldsymbol{\rho}')}{\partial n'} - \frac{1}{2\pi} \left[\log\left(\frac{k\varrho}{2}\right) + \gamma \right] \frac{\partial \psi(\boldsymbol{\rho}')}{\partial n'} + \psi(\boldsymbol{\rho}') \frac{\varrho}{2\pi\varrho^2} \right\} = \psi(\boldsymbol{\rho}), \end{aligned} \quad (\text{A.8})$$

where the following expansions of the Hankel functions for small argument have been employed [14]:

$$H_0^{(1)}(z) \sim 1 + \frac{2i}{\pi} (\log z + \gamma - \log 2); \quad (\text{A.9})$$

$$H_1^{(1)}(z) \sim -\frac{2i}{\pi z}. \quad (\text{A.10})$$

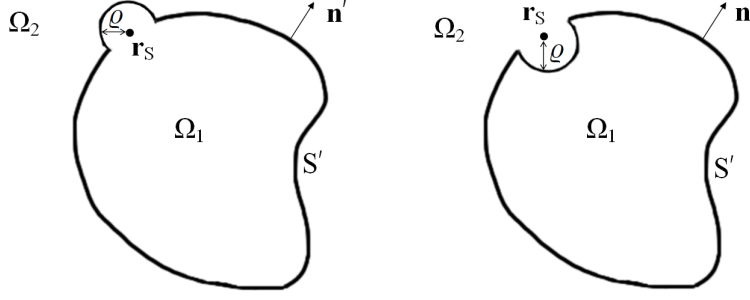


Figure B1. Sketch of two possible deformations of the integration surface.

The three-dimensional case is treated similarly:

$$\begin{aligned}
& \lim_{\varrho \rightarrow 0} \int_{\partial B_{\varrho}(\mathbf{r})} d\mathbf{r}' \left[g^{(3D)} \frac{\partial \psi(\mathbf{r}')}{\partial n'} - \psi(\mathbf{r}') \frac{\partial g^{(3D)}}{\partial n'} \right] \\
&= \lim_{\varrho \rightarrow 0} \int_0^{2\pi} d\phi \int_0^{\pi} d\theta \varrho^2 \sin \theta \left[\frac{\partial \psi(\mathbf{r}')}{\partial n'} - \psi(\mathbf{r}') \left(\frac{ik}{\varrho} - \frac{1}{\varrho^2} \right) \varrho \right] \frac{\exp(ik\varrho)}{4\pi\varrho} = \psi(\mathbf{r}). \quad (\text{A.11})
\end{aligned}$$

Appendix B. Proof of formula (21)

Before taking the limit $\mathbf{r} \rightarrow \mathbf{r}_S$, let us assume to deform the integration surface in the first and second equations of (19) as depicted in the left and right sides of Figure B1, respectively, so that the boundary integrals can be split into two parts:

$$\int_S d\mathbf{r}' = \int_{S - \sigma_{\varrho}(\mathbf{r}_S)} d\mathbf{r}' + \int_{H\partial B_{\varrho}^{\pm}(\mathbf{r}_S)} d\mathbf{r}', \quad (\text{B.1})$$

being $\sigma_{\varrho}(\mathbf{r}_S)$ and $H\partial B_{\varrho}^{\pm}(\mathbf{r}_S)$ a disk and the upper and lower hemispheres of radius ϱ centered at \mathbf{r}_S . In the limit $\varrho \rightarrow 0$, the first term in (B.1) may be replaced by a principal value integral. By writing explicitly the second term in two dimensions, we get:

$$\begin{aligned}
& \lim_{\varrho \rightarrow 0} \int_{H\partial B_{\varrho}^{\pm}(\mathbf{r}_S)} d\mathbf{r}' \left[g^{(2D)}(\mathbf{r}_S, \mathbf{r}') \frac{\partial \psi(\mathbf{r}')}{\partial n'} - \psi(\mathbf{r}') \frac{\partial g^{(2D)}(\mathbf{r}_S, \mathbf{r}')}{\partial n'} \right] \\
&= \lim_{\varrho \rightarrow 0} \int_0^{\pi} d\varphi \varrho \left[\frac{i}{4} H_0^{(1)}(k\varrho) \frac{\partial \psi(\boldsymbol{\rho}')}{\partial n'} - \psi(\boldsymbol{\rho}') \frac{ik H_1^{(1)}(k\varrho)}{4\varrho} (\mp \varrho) \right] = \pm \frac{\psi(\boldsymbol{\rho}_S)}{2}. \quad (\text{B.2})
\end{aligned}$$

Analogously, in three dimensions:

$$\begin{aligned}
& \lim_{\varrho \rightarrow 0} \int_{H\partial B_{\varrho}^{\pm}(\mathbf{r}_S)} d\mathbf{r}' \left[g^{(3D)}(\mathbf{r}_S, \mathbf{r}') \frac{\partial \psi(\mathbf{r}')}{\partial n'} - \psi(\mathbf{r}') \frac{\partial g^{(3D)}(\mathbf{r}_S, \mathbf{r}')}{\partial n'} \right] \\
&= \lim_{\varrho \rightarrow 0} \int_0^{2\pi} d\phi \int_0^{\pi/2} d\theta \varrho^2 \sin \theta \left[\frac{\partial \psi(\mathbf{r}')}{\partial n'} + \psi(\mathbf{r}') \left(\frac{ik}{\varrho} - \frac{1}{\varrho^2} \right) (\mp \varrho) \right] \frac{\exp(ik\varrho)}{4\pi\varrho} = \pm \frac{\psi(\mathbf{r}_S)}{2}. \quad (\text{B.3})
\end{aligned}$$

Appendix C. Proof of formula (28)

By using $\psi_1(\mathbf{r}_S) \equiv \psi(\mathbf{r}_S)$ and $\chi_1(\mathbf{r}_S) \equiv \chi(\mathbf{r}_S)$, system (27) can be rewritten as:

$$\begin{cases} \frac{1}{m_1} \frac{\partial \psi_1(\mathbf{r}_-)}{\partial n_-} = \int_S d\mathbf{r}'_S \frac{\partial g_1(\mathbf{r}_-, \mathbf{r}'_S)}{\partial n_-} \chi(\mathbf{r}'_S) - \frac{1}{m_1} \int_S d\mathbf{r}'_S \frac{\partial^2 g_1(\mathbf{r}_-, \mathbf{r}'_S)}{\partial n_- \partial n'} \psi(\mathbf{r}'_S); \\ \frac{1}{m_2} \frac{\partial \psi_2(\mathbf{r}_+)}{\partial n_+} = \frac{1}{m_2} \int_S d\mathbf{r}'_S \frac{\partial^2 g_2(\mathbf{r}_+, \mathbf{r}'_S)}{\partial n_+ \partial n'} \psi(\mathbf{r}'_S) - \int_S d\mathbf{r}'_S \frac{\partial g_2(\mathbf{r}_+, \mathbf{r}'_S)}{\partial n_+} \chi(\mathbf{r}'_S), \end{cases} \quad (\text{C.1})$$

where $\mathbf{r}_\pm \in S_\varepsilon^\pm$. The procedure described in Appendix B is now applied to the integrals containing a single normal derivative of the Green function, deforming the integration surface and then taking the limit $\varepsilon \rightarrow 0$, so that $S_\varepsilon^\pm \rightarrow S$ and $\mathbf{r}_\pm \rightarrow \mathbf{r}_S$:

$$\int_S d\mathbf{r}'_S \frac{\partial g(\mathbf{r}_S, \mathbf{r}'_S)}{\partial n} \chi(\mathbf{r}'_S) = \oint_S d\mathbf{r}'_S \frac{\partial g(\mathbf{r}_S, \mathbf{r}'_S)}{\partial n} \chi(\mathbf{r}'_S) + \lim_{\varepsilon \rightarrow 0} \int_{H\partial B_\varepsilon^\pm(\mathbf{r}_S)} d\mathbf{r}' \frac{\partial g(\mathbf{r}_S, \mathbf{r}')}{\partial n} \chi(\mathbf{r}'). \quad (\text{C.2})$$

Finally, making use of the result:

$$\lim_{\varepsilon \rightarrow 0} \int_{H\partial B_\varepsilon^+(\mathbf{r}_S)} d\mathbf{r}' \frac{\partial g(\mathbf{r}_S, \mathbf{r}')}{\partial n} \chi(\mathbf{r}') = - \lim_{\varepsilon \rightarrow 0} \int_{H\partial B_\varepsilon^-(\mathbf{r}_S)} d\mathbf{r}' \frac{\partial g(\mathbf{r}_S, \mathbf{r}')}{\partial n} \chi(\mathbf{r}'), \quad (\text{C.3})$$

it is apparent that (28) corresponds to the difference between the two equations in (C.1).

Appendix D. Semi-analytical formulas for the singular integrals in (40)-(43)

Let us introduce the following boundary integral operators:

$$\hat{s}[f](\mathbf{r}_S) \equiv \oint_S d\mathbf{r}'_S g(\mathbf{r}_S, \mathbf{r}'_S) f(\mathbf{r}'_S); \quad (\text{D.1})$$

$$\hat{d}[f](\mathbf{r}_S) \equiv \oint_S d\mathbf{r}'_S \frac{\partial g(\mathbf{r}_S, \mathbf{r}'_S)}{\partial n'} f(\mathbf{r}'_S); \quad (\text{D.2})$$

$$\hat{d}^\dagger[f](\mathbf{r}_S) \equiv \oint_S d\mathbf{r}'_S \frac{\partial g(\mathbf{r}_S, \mathbf{r}'_S)}{\partial n} f(\mathbf{r}'_S); \quad (\text{D.3})$$

$$\hat{n}[f](\mathbf{r}_S) \equiv \int_S d\mathbf{r}'_S \frac{\partial^2 g(\mathbf{r}_S, \mathbf{r}'_S)}{\partial n \partial n'} f(\mathbf{r}'_S) \quad (\text{D.4})$$

and the corresponding Galerkin matrices:

$$s_{ij} \equiv \sum_{m \in i} \sum_{n \in j} \int_{S_m} d\mathbf{r} \int_{S_n} d\mathbf{r}' g(\mathbf{r}, \mathbf{r}') f_i^m(\mathbf{r}) f_j^n(\mathbf{r}'); \quad (\text{D.5})$$

$$d_{ij} \equiv \sum_{m \in i} \sum_{n \in j} \int_{S_m} d\mathbf{r} \int_{S_n} d\mathbf{r}' \frac{\partial g(\mathbf{r}, \mathbf{r}')}{\partial n'} f_i^m(\mathbf{r}) f_j^n(\mathbf{r}'); \quad (\text{D.6})$$

$$d_{ij}^\dagger \equiv \sum_{m \in i} \sum_{n \in j} \int_{S_m} d\mathbf{r} \int_{S_n} d\mathbf{r}' \frac{\partial g(\mathbf{r}, \mathbf{r}')}{\partial n} f_i^m(\mathbf{r}) f_j^n(\mathbf{r}'); \quad (\text{D.7})$$

$$n_{ij} \equiv \sum_{m \in i} \sum_{n \in j} \int_{S_m} d\mathbf{r} \int_{S_n} d\mathbf{r}' \frac{\partial^2 g(\mathbf{r}, \mathbf{r}')}{\partial n \partial n'} f_i^m(\mathbf{r}) f_j^n(\mathbf{r}'). \quad (\text{D.8})$$

Using these definitions, equations (40)-(43) can be rewritten as:

$$S = m_1 s_1 + m_2 s_2; \quad (\text{D.9})$$

$$D = d_1 + d_2; \quad (\text{D.10})$$

$$D^\dagger = d_1^\dagger + d_2^\dagger; \quad (\text{D.11})$$

$$N = \frac{n_1}{m_1} + \frac{n_2}{m_2}, \quad (\text{D.12})$$

where labels 1, 2 refer to the inner and outer regions, respectively, and the matrix indices have been neglected to avoid confusion.

Limiting the analysis to the two-dimensional case, where the piecewise smooth closed curve S is discretized into a collection of segments $\{S_n\}$ with lengths $\{l_n\}$ and extrema $\{\mathbf{r}_A^n; \mathbf{r}_B^n\}$, we can consider first-order basis functions:

$$f_j^n(t_n) \equiv \begin{cases} 1 - t_n & \text{if } \mathbf{r}_j = \mathbf{r}_A^n; \\ t_n & \text{if } \mathbf{r}_j = \mathbf{r}_B^n, \end{cases} \quad (\text{D.13})$$

being $\mathbf{r}_j = (x_j, y_j)$ the position of the j -th mesh node and $t_n \in [0, 1]$ a local parameter for the n -th segment such that:

$$\mathbf{r}(t_n) = \mathbf{r}_A^n + (\mathbf{r}_B^n - \mathbf{r}_A^n) t_n. \quad (\text{D.14})$$

Each of the discrete operators \mathbf{s}_{ij} , \mathbf{d}_{ij} , \mathbf{d}_{ij}^\dagger and \mathbf{n}_{ij} in (D.5)-(D.8) consists of a sum of four double integrals over the pairs of segments $(S_m, S_n) \in \{m \in i\} \times \{n \in j\}$. Whereas all the integrations involving disjoint segments can be computed by Gauss-Legendre quadrature rules, the singular integrals over coincident and adjacent segments deserve special care, as detailed in the following.

Appendix D.1. Singular integrals in (D.5)

When $S_m = S_n$, the singular double integrals in (D.5) can be expressed as:

$$\frac{i}{4} \int_0^{l_n} dx \int_{-x}^{l_n-x} dx' H_0^{(1)}(k|x'|) f_i^n(x) \tilde{f}_j^n(x', x), \quad (\text{D.15})$$

with:

$$f_i^n(x) \equiv \begin{cases} 1 - \frac{x}{l_n} & \text{if } x_i = 0; \\ \frac{x}{l_n} & \text{if } x_i = l_n, \end{cases} \quad (\text{D.16})$$

$$\tilde{f}_j^n(x', x) \equiv \begin{cases} 1 - \frac{(x'+x)}{l_n} & \text{if } x'_j = -x; \\ \frac{(x'+x)}{l_n} & \text{if } x'_j = l_n - x. \end{cases} \quad (\text{D.17})$$

Four kinds of integrals are obtained from (D.15), (D.16) and (D.17), namely:

$$I_a^n \equiv \frac{i}{4} \int_0^{l_n} dx \int_{-x}^{l_n-x} dx' H_0^{(1)}(k|x'|) \left(1 - \frac{x}{l_n}\right) \left[1 - \frac{(x'+x)}{l_n}\right]; \quad (\text{D.18})$$

$$I_b^n \equiv \frac{i}{4} \int_0^{l_n} dx \int_{-x}^{l_n-x} dx' H_0^{(1)}(k|x'|) \left(1 - \frac{x}{l_n}\right) \left[\frac{(x'+x)}{l_n}\right]; \quad (\text{D.19})$$

$$I_c^n \equiv \frac{i}{4} \int_0^{l_n} dx \int_{-x}^{l_n-x} dx' H_0^{(1)}(k|x'|) \left(\frac{x}{l_n}\right) \left[1 - \frac{(x'+x)}{l_n}\right]; \quad (\text{D.20})$$

$$I_d^n \equiv \frac{i}{4} \int_0^{l_n} dx \int_{-x}^{l_n-x} dx' H_0^{(1)}(k|x'|) \left(\frac{x}{l_n}\right) \left[\frac{(x'+x)}{l_n}\right]. \quad (\text{D.21})$$

Making reference to the tabulated formulas for Bessel functions [17], the previous expressions can be reduced to:

$$I_a^n = I_d^n = \frac{i\pi}{8k^2} \left[H_1^{(1)}(kl_n) \mathbf{H}_0(kl_n) - H_0^{(1)}(kl_n) \mathbf{H}_1(kl_n) \right] + \\ - \frac{i}{2k^2} H_2^{(1)}(kl_n) + \frac{2}{\pi k^4 l_n^2} + \frac{i}{4k^2} \Gamma_1(kl_n) + \frac{i}{2k^4 l_n^2} \Gamma_3(kl_n); \quad (\text{D.22})$$

$$I_b^n = I_c^n = -I_a^n + \frac{i}{4k^2} \Gamma_1(kl_n), \quad (\text{D.23})$$

where \mathbf{H}_ν represents the Struve function of order ν and the remaining integrals:

$$\Gamma_1(\sigma) \equiv \frac{\pi}{2} \int_0^\sigma dx x \left[H_0^{(1)}(x) \mathbf{H}_{-1}(x) + H_1^{(1)}(x) \mathbf{H}_0(x) \right]; \quad (\text{D.24})$$

$$\Gamma_3(\sigma) \equiv \frac{\pi}{2} \int_0^\sigma dx x^2 (x - \sigma) \left[H_0^{(1)}(x) \mathbf{H}_{-1}(x) + H_1^{(1)}(x) \mathbf{H}_0(x) \right] \quad (\text{D.25})$$

are left to Gauss-Legendre quadrature formulas.

When the elements S_m and S_n in (D.5) are adjacent, the Green function (A.2) diverges in correspondence of the common vertex. However, since the logarithmic divergence is integrable and the singular end point is not considered, standard Gauss-Legendre quadrature applies.

Appendix D.2. Singular integrals in (D.6) and (D.7)

As follows from the fact that $(\mathbf{r} - \mathbf{r}') \perp \mathbf{n}$ for both \mathbf{r} and \mathbf{r}' lying on the same segment with unit normal \mathbf{n} , all double integrals over coincident segments in (D.6) and (D.7) vanish identically. On the other hand, the only singular contribution to the integrations over adjacent segments is when both $f_i^m(\mathbf{r})$ and $f_j^n(\mathbf{r}')$ are one at the common vertex. In this case, the singularity is stronger than that in the previous section and direct use of Gauss-Legendre quadrature formulas may lead to inaccurate results. A useful technique to improve accuracy consists in introducing a coordinate transformation with vanishing Jacobian at the common vertex to cancel the singularity [11].

Appendix D.3. Singular integrals in (D.8)

Since a direct evaluation of the hypersingular integrals in (D.8) would require explicit cancellation of the logarithmic divergences arising from both coincident and adjacent integrations, an alternative approach based on the variational formulation described in [13, 16] is considered in the present section. We start by writing the bilinear form induced by the hypersingular operator (D.4):

$$\langle \zeta | \hat{\mathbf{n}} | \psi \rangle = \int_S d\mathbf{r} \zeta(\mathbf{r}) \hat{\mathbf{n}}[\psi](\mathbf{r}). \quad (\text{D.26})$$

Then, exploiting the symmetry of the Green function and making use of integration by parts, we have:

$$\hat{\mathbf{n}}[\psi](\mathbf{r}) = \int_S d\mathbf{r}' \text{curl}_S g^{(2D)}(\mathbf{r}, \mathbf{r}') \text{curl}'_S \psi(\mathbf{r}') + k^2 \int_S d\mathbf{r}' g^{(2D)}(\mathbf{r}, \mathbf{r}') \psi(\mathbf{r}') (\mathbf{n} \cdot \mathbf{n}'), \quad (\text{D.27})$$

where:

$$\text{curl}_S \equiv \mathbf{n} \cdot \mathbf{curl} = n_x \frac{\partial}{\partial y} - n_y \frac{\partial}{\partial x} \quad (\text{D.28})$$

and \mathbf{curl} is the surface curl on \mathbb{R}^2 . Using again integration by parts, (D.26) is reduced to:

$$\langle \zeta | \hat{\mathbf{n}} | \psi \rangle = \int_S d\mathbf{r} \int_S d\mathbf{r}' g^{(2D)}(\mathbf{r}, \mathbf{r}') \left[k^2 (\mathbf{n} \cdot \mathbf{n}') \zeta(\mathbf{r}) \psi(\mathbf{r}') - \text{curl}_S \zeta(\mathbf{r}) \text{curl}'_S \psi(\mathbf{r}') \right]. \quad (\text{D.29})$$

If we take $\zeta(\mathbf{r})$ and $\psi(\mathbf{r}')$ to be the basis functions $f_i(\mathbf{r})$ and $f_j(\mathbf{r}')$, we can now replace (D.8) by:

$$n_{ij} = \sum_{m \in i} \sum_{n \in j} \int_{S_m} d\mathbf{r} \int_{S_n} d\mathbf{r}' g^{(2D)}(\mathbf{r}, \mathbf{r}') \left[k^2 (\mathbf{n} \cdot \mathbf{n}') f_i^m(\mathbf{r}) f_j^n(\mathbf{r}') - \text{curl}_{S_m} f_i^m(\mathbf{r}) \text{curl}'_{S_n} f_j^n(\mathbf{r}') \right]. \quad (\text{D.30})$$

In order to apply the curl_S operator to (D.13), the parameterization (D.14) is lifted into the two-dimensional tubular neighborhood of the n -th segment:

$$\mathbf{r}_\varepsilon(t_n) = \mathbf{r}_A^n + (\mathbf{r}_B^n - \mathbf{r}_A^n) t_n + \varepsilon \mathbf{n}. \quad (\text{D.31})$$

Then, taking the inner product of (D.31) with $(\mathbf{r}_B^n - \mathbf{r}_A^n)$, we can write:

$$f_j^n(\mathbf{r}) \equiv \begin{cases} 1 - \frac{1}{l_n^2} (\mathbf{r} - \mathbf{r}_A^n) \cdot (\mathbf{r}_B^n - \mathbf{r}_A^n) & \text{if } \mathbf{r}_j = \mathbf{r}_A^n; \\ \frac{1}{l_n^2} (\mathbf{r} - \mathbf{r}_A^n) \cdot (\mathbf{r}_B^n - \mathbf{r}_A^n) & \text{if } \mathbf{r}_j = \mathbf{r}_B^n. \end{cases} \quad (\text{D.32})$$

Equation (D.32) provides a constant extension of the functions (D.13) along \mathbf{n} . On using (D.28) and the definition of unit normal to the n -th segment in \mathbb{R}^3 , it follows that:

$$\text{curl}_{S_n} f_j^n = \begin{cases} -\frac{1}{l_n} & \text{if } \mathbf{r}_j = \mathbf{r}_A^n; \\ \frac{1}{l_n} & \text{if } \mathbf{r}_j = \mathbf{r}_B^n. \end{cases} \quad (\text{D.33})$$

All the integrations in (D.30) can now be computed as in Appendix D.1. In particular, Gauss-Legendre quadrature formulas directly apply whenever $S_m \neq S_n$. Conversely, the four possible integrals over coincident segments acquire the following form:

$$\tilde{I}_a^n = \tilde{I}_d^n = k^2 I_a^n - \frac{1}{l_n^2} \int_{S_n} d\mathbf{r} \int_{S_n} d\mathbf{r}' g^{(2D)}(\mathbf{r}, \mathbf{r}') = k^2 I_a^n - \frac{i}{2k^2 l_n^2} \Gamma_1(kl_n); \quad (\text{D.34})$$

$$\tilde{I}_b^n = \tilde{I}_c^n = k^2 I_b^n + \frac{1}{l_n^2} \int_{S_n} d\mathbf{r} \int_{S_n} d\mathbf{r}' g^{(2D)}(\mathbf{r}, \mathbf{r}') = k^2 I_b^n + \frac{i}{2k^2 l_n^2} \Gamma_1(kl_n), \quad (\text{D.35})$$

where I_a^n, I_b^n and $\Gamma_1(kl_n)$ are defined in (D.22)-(D.24) and the tilde is to avoid notation overlap.

Appendix E. Calderon preconditioning of (39)

The boundary integral operators (D.1)-(D.4) can be shown to satisfy the Calderon relations [13]:

$$\hat{\mathbf{d}} \hat{\mathbf{s}} = \hat{\mathbf{s}} \hat{\mathbf{d}}^\dagger; \quad (\text{E.1})$$

$$\hat{\mathbf{n}} \hat{\mathbf{d}} = \hat{\mathbf{d}}^\dagger \hat{\mathbf{n}}; \quad (\text{E.2})$$

$$\hat{\mathbf{d}}^2 - \hat{\mathbf{s}} \hat{\mathbf{n}} = \hat{I}/4; \quad (\text{E.3})$$

$$\hat{\mathbf{d}}^{\dagger 2} - \hat{\mathbf{n}} \hat{\mathbf{s}} = \hat{I}/4, \quad (\text{E.4})$$

with \hat{I} representing the identity operator. After discretizing the boundary S , both sides of (D.1)-(D.4) can be expanded on a set of node-based basis functions $\{f_j\}$. Let us consider, for instance, equation (D.1):

$$\hat{\mathbf{s}}[f](\mathbf{r}_S) = \sum_j \alpha_j f_j(\mathbf{r}_S); \quad f(\mathbf{r}'_S) = \sum_j \beta_j f_j(\mathbf{r}'_S). \quad (\text{E.5})$$

Applying the Galerkin method, we obtain:

$$\sum_j F_{ij} \alpha_j = \sum_j s_{ij} \beta_j \quad (\text{E.6})$$

being F the Gram matrix defined in (114) and \mathbf{s} the discrete operator in (D.5). The same procedure can be used to discretize the other operators and their products, leading to the following matrix version of (E.1)-(E.4):

$$\mathbf{F}^{-1} \mathbf{h} \mathbf{F}^{-1} \mathbf{h} = \mathbf{I}/4, \quad (\text{E.7})$$

where:

$$\mathbf{h}_{ij} \equiv \begin{pmatrix} -\mathbf{d}_{ij} & \mathbf{s}_{ij} \\ -\mathbf{n}_{ij} & \mathbf{d}_{ij}^\dagger \end{pmatrix}; \quad \mathbf{F}_{ij} \equiv \begin{pmatrix} F_{ij} & 0 \\ 0 & F_{ij} \end{pmatrix}. \quad (\text{E.8})$$

Using (E.7), (D.9)-(D.12) and (39), it can be shown that [18]:

$$\mathbf{H}\mathbf{F}^{-1}\mathbf{H}\mathbf{F}^{-1} \approx \mathbf{I} + \mathbf{C}, \quad (\text{E.9})$$

with \mathbf{C} resulting from the discretization of a compact operator. Therefore, the block matrix \mathbf{F} can be employed as a right preconditioner in both (88) and (113).

- [1] Balkanski M and Wallis R F 2000 *Semiconductor Physics and Applications* (Oxford University Press)
- [2] Harrison P and Valavanis A 2016 *Quantum Wells, Wires and Dots* 4th ed (John Wiley and Sons, Inc., Chichester, West Sussex, UK)
- [3] Böer K W and Pohl U W 2018 *Semiconductor Physics* (Springer, Berlin)
- [4] Kulik I O and Ellialtıođlu R 2000 *Quantum Mesoscopic Phenomena and Mesoscopic Devices in Microelectronics* (Springer Science and Business Media, Dordrecht)
- [5] Knipp P A and Reinecke T L 1996 *Physical Review B* **54**(3) 1880–1891 URL <https://link.aps.org/doi/10.1103/PhysRevB.54.1880>
- [6] Gelbard F and Malloy K 2001 *Journal of Computational Physics* **172** 19 – 39 URL <http://www.sciencedirect.com/science/article/pii/S0021999101967518>
- [7] Ram-Mohan L R 2002 *Finite Element and Boundary Element Applications in Quantum Mechanics* (Oxford University Press)
- [8] Cai W 2013 *Computational Methods for Electromagnetic Phenomena* (Cambridge University Press)
- [9] Sun Q, Klaseboer E, Khoo B-C and Chan D Y C 2015 *Royal Society Open Science* **2**(1) 140520 URL <https://royalsocietypublishing.org/doi/abs/10.1098/rsos.140520>
- [10] Klaseboer E, Sepehriraahnama S and Chan D Y C 2017 *The Journal of the Acoustical Society of America* **142**(2) 697–707 URL <https://doi.org/10.1121/1.4996860>
- [11] Sutradhar A, Paulino G H and Gray L J 2008 *Symmetric Galerkin Boundary Element Method* (Springer-Verlag Berlin Heidelberg)
- [12] Lévy-Leblond J M 1995 *Physical Review A* **52**(3) 1845–1849
- [13] Nédélec J C 2001 *Acoustic and Electromagnetic Equations* (Springer-Verlag New York, Inc.)
- [14] Abramowitz M and Stegun I A 1972 *Handbook of Mathematical Functions* 10th ed (Washington, DC: National Bureau of Standards, US Government Printing Office)
- [15] Wilton D, Rao S, Glisson A, Schaubert D, Al-Bundak O and Butler C 1984 *IEEE Transactions on Antennas and Propagation* **32** 276–281
- [16] Steinbach O 2008 *Numerical Approximation Methods for Elliptic Boundary Value Problems* (Springer, New York)
- [17] Gradshteyn I S and Ryzhik I M 2007 *Table of Integrals, Series, and Products* 7th ed (Academic Press, Elsevier, USA)
- [18] Niino K and Nishimura N 2012 *Journal of Computational Physics* **231** 66–81 URL <http://www.sciencedirect.com/science/article/pii/S0021999111005067>